

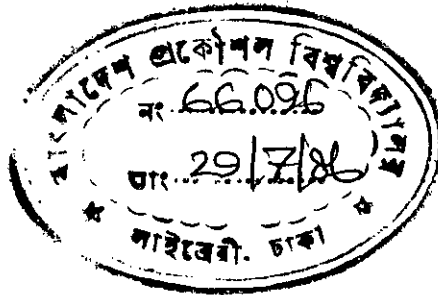
A STUDY OF INDUCED FLOW DEVELOPMENT ALONG THE DOWNSTREAM  
OF AN AXISYMMETRIC JET ISSUING AXIALLY INTO A SMOOTH PIPE

by

R.G.M. HASAN

B.Sc.Engg. (Mech.)

Thesis submitted to the  
Department of Mechanical Engineering in partial fulfilment  
of the requirements for the degree of  
Master of Science  
in  
Mechanical Engineering



Bangladesh University of Engineering and Technology  
Dhaka Bangladesh

December 1985



#66096#

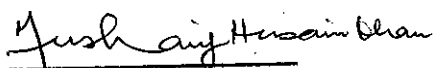
A STUDY OF INDUCED FLOW DEVELOPMENT ALONG THE DOWNSTREAM  
OF AN AXISYMMETRIC JET ISSUING AXIALLY INTO A SMOOTH PIPE

A Thesis

by

R.G.M. Hasan.

Approved as to style and content:



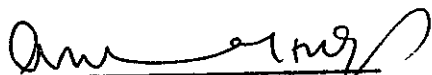
(Dr. M.H. Khan)  
Professor,  
Dept. of Mechanical Engg.,  
BUET, Dhaka.

Chairman



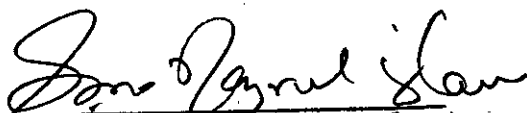
(Dr. M.A. Taher Ali)  
Professor and Head,  
Dept. of Mechanical Engg.,  
BUET, Dhaka.

Member



(Dr. A. M. Aziz-ul Haq)  
Professor,  
Dept. of Mechanical Engg.,  
BUET, Dhaka.

Member



(Dr. S.M. Nazrul Islam)  
Professor,  
Dept. of Mechanical Engg.,  
BUET, Dhaka.

Member



(Dr. Abdul Hannan)  
Professor,  
Dept. of Water Resources Engg.,  
BUET, Dhaka.

Member  
(External)

Candidate's Declaration

It is hereby declared that neither this thesis nor any part thereof has been submitted or is being concurrently submitted anywhere for the award of any degree or diploma or publication.

*R. G. M. Ham*

Candidate

## ABSTRACT

The flow characteristic along the downstream of an axisymmetric jet issuing axially into a smooth pipe was studied experimentally. For this purpose, a basic experimental facility was designed, fabricated and installed.

The boundary layer thickness of the velocity profile at jet exit was varied by using three nozzles of different surfaces. One was smooth and the other two had relative surface roughnesses of  $\epsilon/D_n = 1/70$  and  $\epsilon/D_n = 1/20$ . Mean axial velocity and static pressure were measured along the mixing pipe at Reynolds numbers  $2.39 \times 10^4$ ,  $3.28 \times 10^4$ ,  $4.24 \times 10^4$  and  $5.51 \times 10^4$ . The Reynolds number was defined on the basis of diameter of the nozzle and the area-mean velocity at nozzle exit.

The variation of static pressure along the mixing pipe (upto 44 diameters) was studied and the maximum pressure rise was compared with a theoretical model. The maximum pressure was observed near the section where the jet attached to the wall. The rate of induced flow was determined for different Reynolds number and boundary layer thickness at nozzle exit. The maximum induced

flow was found to be 21.95% and it occurred at  $Re_n = 3.28 \times 10^4$  and nozzle roughness of  $\epsilon/D_n = 1/20$ . The zone of attachment of the jet with pipe wall was found to be between  $x/r_t = 5.5$  to 7.5. A possible recirculation was identified at the initial region of the pipe. Variation of centre line velocities along the pipe was also studied. It was found from the experiment that after the jet attached to the wall, the flow pattern along the downstream was a developing turbulent pipe flow.

## ACKNOWLEDGEMENTS

With deep sincerity, the author acknowledges profound indebtedness to his supervisor Dr. Musharrif Hussain Khan, Professor, Department of Mechanical Engineering for his guidance, constant encouragement and invaluable suggestion in achieving every minute detail of this thesis.

The author feels highly grateful to Dr. M.A. Taher Ali, Professor and Head, Department of Mechanical Engineering, BUET who provided all necessary assistance in various ways at different stages of the work.

The helpful suggestions by Dr. S.M. Nazrul Islam and Dr. Dipak Kanti Das, Professors of Mechanical Engineering department are very much appreciated.

The inspirations and suggestions shown by Professor A.M. Aziz-ul Huq of Mechanical Engineering department and Professor A.F.M. Anwarul Haque of Industrial and Production Engineering department during the thesis are also highly appreciated.

Sincere thanks are offered to Mr. Ahmed Ali Mollah, Chief Foreman Instructor, Machine Shop, BUET and Mr. Julfikar Ali Bhuiyan, Chief Supervisor, Welding and Sheet Metal Shop,

BUET, for their kind cooperation in the construction of the experimental set up.

Finally the author expresses his thanks to all of his colleagues in Mechanical Engineering department and members of his family for their cooperation and inspiration during the work.

To My Parents



## TABLE OF CONTENTS

	<u>Page</u>
Title	ii
Certificate of Approval	iii
Candidate's Declaration	iv
Abstract	v
Acknowledgements	vii
Dedication	ix
Table of Contents	x
List of Nomenclature	xiii
 CHAPTER - I INTRODUCTION	
1.1 General	1
1.2 Axisymmetric Turbulent Jet and Induced Flow	2
1.3 Importance of Confined Jets	3
1.4 Objectives	4
 CHAPTER -II LITERATURE SURVEY	
2.1 General	6
2.2 Confined Jets	6
2.2.1 The Initial Region	10
2.2.2 The Duct Flow Region	15
 CHAPTER -III THEORY	
3.1 General	16
3.2 Definition of Parameters	16
 CHAPTER -IV EXPERIMENTAL SET UP AND PROCEDURE	
4.1 General	19

	<u>Page</u>
4.2 The Jet Producing Section	19
4.3 The Test Section	21
4.4 Flow Measuring Devices	22
4.4.1 The Inlet Nozzle	23
4.4.2 The Orifice Meter	23
4.5 Alignment and Positioning of the Set Up	24
4.6 Measurement of Velocity Profile and Static Pressure	25
4.7 Procedure of Measurement	26
4.8 Error Analysis	28
 CHAPTER-V RESULTS AND DISCUSSIONS	
5.1 General	29
5.2 Exit Conditions of the Jet	29
5.3 Mean Velocity Profiles	31
5.4 Axial Pressure Gradient	32
5.5 Wall Shear Stress	33
5.6 Growth of the Jet and Attachment	33
5.7 Variation of Centre Line Velocity	34
5.8 Induced Mass Flow Rate	35
5.9 Comparison of Excess Velocity Profiles	36
 CHAPTER-VI CONCLUSION	
6.1 General	37
6.2 Findings of the Present Work	37
6.3 Limitations of the Study	39
6.4 Extensions of the Present Work	39

	<u>Page</u>
APPENDIX- A Determination of Wall Shear Stresses	42
APPENDIX- B Determination of Maximum Pressure Rise	44
APPENDIX- C Uncertainty Analysis for Mean Quantity Measurements	47
REFERENCES	55
LIST OF FIGURES	60
FIGURES	61
LIST OF PLATES	93
PLATES	94

LIST OF NOMENCLATURE

Symbol	Meaning
Latin letters:	
A	Cross sectional area
$C, C', C_1, C_2$	Constants
Cd	Coefficient of discharge
CT	Craya-Curtet number
D	Diameter
f	Friction factor
g	Acceleration due to gravity
H	Shape factor
$k_1, k_2$	Constants
$\dot{M}$	Induced flow rate in percent
m	Similitude parameter = $1/CT^2$
$\dot{m}$	Mass flow rate
p	Mean static pressure
$P^*$	Non-dimensional pressure rise = $(p-p_o)/\rho\bar{U}_o^2$
r	Radius
$r_{\frac{1}{2}}$	Half-velocity radius i.e., radius at which $(u-u_s) = 0.5(u_c-u_s)$
u	Local axial mean velocity
U	Free stream velocity, Velocity at potential core
$\bar{U}$	Area-mean velocity

Symbol	Meaning
x	Axial distance measured from the exit plane of the jet-nozzle
X	Nondimensional axial distance= $x/r_t$
y	Vertical distance measured from the wall

## Greek letters:

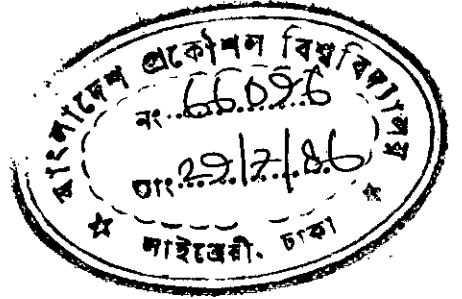
$\rho$	Density of the fluid
$\mu$	Absolute viscosity of fluid
$\nu$	Kinematic viscosity
$\tau$	Shear stress
$\epsilon$	Average roughness height
$\delta$	Boundary layer thickness
$\delta^*$	Displacement thickness
$\theta$	Momentum thickness
$\phi$	Phase of AC supply

## Subscripts:

a	at atmospheric condition
c	at centre line
n	of jet nozzle
o	at inlet plane of the mixing pipe
p	of primary jet flow
pc	of potential core
s	of secondary stream
t	of mixing pipe
w	at wall

## CHAPTER - I

### INTRODUCTION



#### 1.1 General

Jets are formed when a fluid is discharged through an opening from a region at a higher pressure to a region of lower pressure. If the jet is allowed to expand in an infinite fluid it is termed a free jet. On the other hand, if it impinges on a rigid wall it is called a wall jet. When a free jet is bounded by a conduit it is known as a confined jet.

Like the other two types, confined jet has got some practical importance in different industrial and engineering applications. These jets are mostly turbulent in nature and the flow development pattern along the downstream of the jet has been the object of research for many years. Since the governing equations for turbulent flows are quite complicated, and analytical solutions are difficult; empirical equations and correlations have been developed for its prediction. By employing numerical techniques the governing equations for turbulent flows may be solved by using fast computers, and the calculated results need verification by experiments.

## 1.2 Axisymmetric Turbulent Jet and Induced Flow

Axisymmetric jets are those in which the average value of any function of velocities and of their derivatives is invariant under rotations about an axis in the given direction and under reflections with respect to planes through this axis and perpendicular to it. Such a jet can be produced by forcing a fluid through a streamlined nozzle having a circular opening. For turbulent jets it has been observed by flow visualization technique that perturbations are present at the periphery of the nozzle outlet, which grow with distance from the jet exit (32)\*. These perturbations take the form of vortices and eddies in the axial direction and those in contact with the ambient fluid fold back and thus entrain the surrounding fluid. The mass flow rate within the jet increases downstream with a decrease in velocity. For an axisymmetric turbulent jet issuing axially into a smooth pipe having diameter larger than that of the nozzle at exit, the entrainment process occurs upto the point where the jet strikes the wall boundary. This phenomenon causes a secondary flow to be induced into the larger diameter pipe hereinafter referred to as the mixing pipe. The amount of induced flow

\*numbers in parenthesis refer to the serial number in the reference list.

depends on the factors viz., the ratio of diameters of the mixing pipe and the nozzle outlet, the Reynolds number, the boundary layer of the velocity profile at nozzle exit and the location of the exit plane of the jet with respect to the inlet section of the mixing pipe, if the fluctuations of velocity and pressure are not considered.

The type of flow discussed in the previous paragraph can be divided into two principal regions: 1) The initial region and 2) The duct flow region. The initial region extends from the exit of the jet to the point where it reaches the wall. On the other hand, the duct flow region starts after the jet attaches the wall. In this region the velocity profile changes with axial distance and the effect of the jet cannot be identified. Ultimately the flow is expected to become fully developed turbulent flow through a pipe.

### 1.3 Importance of Confined Jets

The use of jet pumps dates back to as early as 1852 when James Thomson (39) used it for the first time for the specific purpose of removing water from the pits of submerged water wheels. Later the induced flow of confined jets had been in use in the fuel injection



system of diesel engines and is still used in the fuel spraying in boiler furnaces. In air-conditioning plants the steam-jet ejectors are used. Water jet pumps employing the principle of confined jet and induced flow include deep well pumping, booster pumping, dredging, tail water suppressors, priming devices etc. In ordinary gas burners, natural gas comes out in the form of jet which is enclosed coaxially within a converging-diverging mixing duct. The air inducted mixes with the gas in proper proportions. In some furnaces the flame is controlled by providing a coaxial stream.

The field of confined jets is thus very important from a practical view point and therefore, the subject has been studied by many researchers.

#### 1.4 Objectives

Considering the different applications of the confined jets and its importance as discussed in the preceding section a research scheme has been undertaken. A suitable experimental set up has been designed, fabricated and installed to study the flow behaviour along the downstream of axisymmetric jets in a pipe. The flow variables such as mean velocities and static pressures at

different sections of the mixing pipe are to be measured. The Reynolds number and the boundary layer of the velocity profile at the exit of the nozzle will be varied. The specific objectives of the present work are enumerated below:

1. To study the effect of Reynolds number and boundary layer of the velocity profile at nozzle exit on the induced flow.
2. To study the effect of Reynolds number and boundary layer of the velocity profile on the attachment of the jet with pipe wall.
3. To study the flow development along the downstream.
4. To study the static pressure distributions along the pipe and to compare the maximum pressure rise with a theoretical equation.
5. To compare the findings and observations with the available information in the literature.

## CHAPTER - II

### LITERATURE SURVEY

#### 2.1 General

Many authors have studied the flow characteristic of jets with different fluids under different geometrical configurations. But the volume of work involving air jets are much larger than those with other fluids. The possible reasons are: (a) study of air jets can be utilised to describe the behaviour of jets with other fluids and (b) ease of handling of the experiment in a common research laboratory. These jets, as already mentioned, are of three types: free, confined and wall jets. Out of these three, free jet flow is the most popular area of research among the scientists and is an established field of Fluid Mechanics (14,36, 40). On the other hand, though the applications of confined jet began since more than a century ago, the number of works in this field is comparatively small.

#### 2.2 Confined Jets

Confined jets that are used in practices are mostly turbulent in nature. The works on these jets can be broadly classified into two groups i.e., theoretical and experimental. The theoretical studies involve the solution of mass flow equation, Navier-Stokes equation, Energy equation, Reynolds stress equation, Length scale equation with

approximate boundary conditions together with the empirical shear stress model. With the advent of very fast computers, researchers have been attracted to theoretical prediction of flow characteristic. But the theoretical findings must be supported by experimental results.

The studies of confined jets have been conducted by many investigators with a large number of flow variables and various geometries. In most cases primary and secondary flows are the main subjects of investigation. The secondary flow surrounds the primary flow and gradually mixes with it in the downstream. In the downstream of the mixing duct the flow development is largely influenced by the relative strengths of these two flow-streams. Advantages of the forced secondary flow are that the ratio of  $\bar{U}_{p,0}/\bar{U}_{s,0}$  can be controlled and experiments can be conducted over a wide range of flow-ratios. On the other hand, induced flow depends on many factors like initial conditions of primary jet, ratio of jet diameter to mixing pipe, entry geometry of mixing pipe, ambient conditions etc. The relative weightage of the two streams is one of the most important parameters in connection with the study of confined jets. A non-dimensional number, the Craya-Curtet number (CT) as proposed by Becker, Hottel and Williams (6)

has been shown to be an index of the relative weightage of streams (Eqn. 3.7). Many authors such as, Hill (19), Exley and Brighton (13), Barchilon and Curtet (3), Razinsky and Brighton (31) used this number as an index of relative weightage of streams. A similitude parameter,  $m = \frac{1}{CT}^2$  is also popular to the scientists. Brighton (12) has, however, shown that CT alone is not a suitable parameter to describe the flow patterns, especially when flow separation and consequent reattachment is encountered. Becker (31) modified the definition of Craya-Curtet number and proposed a more generalized definition of the number by combining the density, momentum flux and mass flux of both the secondary and primary streams. This definition of CT was, however, not very widely accepted by many authors working with confined jet flow.

The orientation of the primary jet and of the mixing duct is very important in the analysis. The most common and the simplest one is when a circular jet is expanded coaxially into a smooth circular pipe. Other types of geometry include the double concentric jets, incident or parallel jets, swirling jets etc., issuing into a duct. The mixing duct is normally a smooth pipe or a rectangular duct of constant cross-sectional area or it can be a convergent-divergent duct (19,21).

The other geometrical variable is the ratio of the jet exit diameter to mixing pipe diameter. Its value varies from zero, when the jet is assumed to be issuing out from a point source, to 0.5 (Table 2.1). The rate of induced flow is largely influenced by the area-ratio. It has been found from experiments that jet pumps (27) with area ratio more than 0.2 show high efficiencies.

The static pressure variation along the mixing pipe is studied by many authors (6,19,21,31) working on confined jet flows (Table 2.1). For smooth mixing tube having constant cross-sectional area static pressure increases in the initial region but decreases after the jet attaches the wall and is not very much sensitive to CT. Whereas for a confined jet in converging-diverging mixing duct, the static pressure variation is distinctly different (21) from that for constant diameter mixing duct. The variation of static pressure has been found to be very much influenced by the value of CT. At lower values there is a substantial depression at the throat. This depression decreases as CT increases and assumes a rising pattern at still higher values of the number. When the secondary flow is an induced one, the static pressure in the initial region shows a negative value which is an indication of suction from ambient fluid (3).

The flow regimes along the downstream of the confined jet can be broadly classified into two parts. The initial region and the region after the shear layer attaches the duct wall (Duct flow region). The relevant works on these flow regions are reviewed in the following two articles.

### 2.2.1 The Initial Region

Length of the initial region is influenced by Reynolds number and the dimensions of primary jet and mixing pipe. This region can be identified as a zone of free jet flow in a moving stream with a positive pressure gradient along the downstream of the mixing duct. Much work has been done both theoretically and experimentally on the free jet flows by Wygnanski (41), Heskestad (18), Newman (28), Townsend (40), Roshko (32), Bradshaw (8), Boguslawski and Popiel (7) and others. In 1977, Chassing (9) in a detailed literature review stated that the free turbulent jet has been investigated by several experimentalists and it is well known for a long time that some region of universal self preserving profiles can be reached at a suitable distance from the exit. This review reveals that the influence of the initial conditions does not distinctly affect the flow behaviour on the downstream of the flow.

Whereas for a confined jet issuing axially into a smooth pipe, the initial region is very much different from that of free jet flow. The negative pressure at the inlet section of mixing pipe causes a secondary stream to be induced into the mixing duct, and the mixing process continues upto the point where the jet attaches the wall of the mixing pipe or an earlier section depending on the Craya-Curtet number. In an experiment carried out by Hill (20), where the ratio of mixing duct diameter to that of the jet exit was 2.5 and the jet exit Reynolds number was  $2.6 \times 10^5$ , the secondary induced flow was found to be 0.3 lb/s, the primary jet flow being 0.2 lb/s.

Studies conducted in the initial region by Exley and Brighton (13), Mikhail (26), Hill (21,22), Habib and Whitelaw (15) have clearly revealed a zone of recirculation before the jet attaches the wall of the mixing pipe.

The behaviour of an axisymmetric jet with recirculation (backflow) was investigated thoroughly both theoretically as well as experimentally by Barchilon and Curtet (3). The study revealed that the approximate confined jet theory (11) proposed by Curtet is applicable to the case of axisymmetric jet with backflow. The authors used bubble injection apparatus to visualize the zone of recirculation.



They also deduced the mean streamline pattern from hot-wire measurements of mean velocity. Later, this backflow has been analyzed theoretically by Hill (19) both for a uniform and a non-uniform duct. If the entrainment rate is high enough the jet entrains all the secondary stream before it (jet) has reached the wall. Downstream of the position of complete entrainment, a recirculation eddy is formed; within the eddy the flow near the wall is reversed. The jet entrains fluid from the upstream part and rejects to the downstream side. The Craya-Curtet number as has been proposed by some authors (19) gives a criterion for the existence or initiation of recirculation. According to Becker, Hottel and Williams (6) if  $CT$  falls below 0.8, recirculation will occur; if it is more than 2 which means that the primary jet is very prominent, the chance of recirculation is very little.

Table 2.1 (19) Experimental Investigations of Confined Jet Flows in Axisymmetric Ducts with Uniform-Density Fluid ( Ducts of uniform cross-sectional area).

Author	Radius ratio $r_n/r_{tw}$	Velocity Ratio $u_{p,o}/u_{s,o}$	CT	$Re_n \times 10^{-4}$	Measurements (a)									
					1	2	3	4	5	6	7	8		
Acharya	.0625	2 - 5	3.6-11.4	2	*					*				
Barchilon & Curtet	.074	15-175, $\infty$	.074-.97	15	*	*	*				*			
Becker, Hottel & Williams	.032	3-200, $\infty$	.032-.1.22	5	*	*	*	*	*				*	
Chen	.2, .5	2, 4	1.16- 3.7	5	*			*	*					
Curtet & Ricou	.074	2-11.5	1.3-11	5	*	*	*			*				*
Dealy	.25, .5	1.5-12, $\infty$	.25- 1.54	5	*					*				
Exley & Brighton	.167, .333	5-53	.35-1.0	Not Mentioned										*
Fejer	.167	2 - 5	1.5 - 4.4	10	*						*			
Forstall & Shapiro	.0625	2 - 5	3.6 -11.4	2	*					*				

Table 2.1(19) (Continued)

Author	Radius Ratio $r_n/r_{tw}$	Velocity Ratio $u_{p,o}/u_{s,o}$	CT	$Re_n \times 10^{-4}$	Measurements (a)								
					1	2	3	4	5	6	7	8	
Helmbold, Leu- sen & Heinrich	.099	7 - 50	.31-1.43	18				*	*				
Hill	.10	7 - 66	.26-1.74	20	*			*					
Razinsky & Brighton	.167	1.5-10	.65 - 2.6	15	*			*	*				*
Mikhail	.26	5	1.1	10	*			*	*				

(a) For variation with axial distance: 1. Centre line velocity 2. Outer Stream Velocity  
 3. Jet radius 4. Static pressure 5. Velocity profiles  
 6. Streamlines 7. Recirculation 8. Turbulent quantities.

### 2.2.2 The Duct Flow Region

When a jet attaches to a wall it begins to undergo considerable changes in its velocity and shear stress distributions. The rate of mixing increases, which is evident from the increased rates of pressure rise and decay of the excess velocity (difference between the local velocity and the secondary induced velocity).

Hill (21,22) has analysed the flow situation in this range by the integral technique with the help of continuity and momentum equations. In this study the mixing pipe was of constant cross-sectional area and data were taken upto about 14 diameters on the downstream side.

The length of the duct on the downstream side up to which the effect of the initial conditions is present, depends on the flow characteristics of the primary and secondary streams. But under all the flow configuration, when the effect of the jet is no more in existence, the flow becomes a pipe flow with a developing velocity profile. This type of turbulent flow, due to its great practical importance, has been studied by many authors in very detailed form(35,36.& 37), and it is now an established field of fluid mechanics.

## CHAPTER - III

### THEORY

#### 3.1 General

In this chapter the basic definitions of boundary layer parameters and of velocity profiles in connection with the present study are introduced.

#### 3.2 Definition of Parameters

The velocity profile at the nozzle exit has an inner constant velocity zone known as the potential core. This core is surrounded by a shear layer (thickness  $\delta$ ) around it. The velocity in the boundary layer decreases gradually from the centre line and assumes zero value at the wall.

The displacement thickness  $\delta^*$  of the boundary layer is the distance the actual boundary would have to be displaced in order that the actual flow rate would be the same as that of an ideal fluid past the displaced boundary. Hence

$$U\delta^* = \int_0^{\delta} (U-u) dy$$
$$\delta^* = \int_0^{\delta} (1-u/U) dy \quad \dots \quad (3.1)$$

The momentum thickness  $\theta$  of the boundary layer is the distance from the actual boundary such that the momentum

flux through the distance  $\theta$  is the same as the deficit of the momentum flux through the actual boundary layer.

Thus

$$(\rho\theta U) U = \int_0^{\delta} \rho(U-u)u \, dy$$

$$\theta = \int_0^{\delta} (u/U)(1-u/U) \, dy \quad \dots \quad (3.2)$$

The ratio of the displacement thickness and the momentum thickness gives the shape factor of the shear layer

$$H = \delta^*/\theta \quad \dots \quad (3.3)$$

The average mean velocity at any cross-section is found from the following equation

$$\bar{U} = (U/A) \int (u/U) \, dA \quad \dots \quad (3.4)$$

The Reynolds number at jet exit is based on the area-mean velocity and the nominal diameter  $D_n$  at the jet exit. Hence

$$Re_n = \frac{\bar{U}_n D_n}{\nu} \quad \dots \quad (3.5)$$

The induced flow rate  $\dot{M}$  is defined as the amount of mass of air inducted by the primary jet in percentage of it. That is

$$M = \frac{\dot{m}_t - \dot{m}_n}{\dot{m}_n} \times 100 \quad \dots (3.6)$$

where  $\dot{m}_t$ ,  $\dot{m}_n$  are the mass flow rates of air through the mixing duct and the nozzle respectively.

The Craya- Curtet number CT, which is a nondimensional measure of the relative weightage of the jet momentum is defined as

$$CT = \frac{\int_{A_0} u \, dA_0}{\left[ A_0 \int_{A_0} u^2 \, dA_0 - \frac{1}{2} A_0^2 \bar{u}_{s,0}^2 - \frac{1}{2} \left( \int_{A_0} u \, dA_0 \right)^2 \right]^{\frac{1}{2}}} \quad (3.7)$$

The above definition of CT has been obtained from  $CT = 1/\sqrt{m}$ , where  $m$  is a similitude parameter derived from the continuity and momentum equations applied for an axisymmetric jet confined within a duct (3). This ( $m$ ) can also be obtained by applying Euler's theorem between two suitable sections of the mixing pipe (3). The parameter  $m$  is a non-dimensional measure of the weighted momentums of the primary and secondary streams. For example, at a given initial jet velocity  $m$  decreases with increasing ambient velocities, and if both the jet and the ambient velocities are same,  $m = 0$  i.e.,  $CT = \infty$ . When the nozzle diameter is very small compared to the pipe diameter, the similitude parameter alone can be found to govern the mixing conditions in the duct.

## C H A P T E R - I V

### EXPERIMENTAL SET UP AND PROCEDURE

#### 4.1 General

An experimental set up was designed, fabricated, and installed. The schematic diagram is shown in figure 4.1. The components were either available in the department or were made from locally available materials. The whole set up can be divided into three parts: 1) The Jet Producing Section. 2) The Test Section and 3) The Flow Measuring Devices.

#### 4.2 The Jet Producing Section

This section consisted of five components, viz., the blower, the settling chamber, the flow straightening section, the converging nozzle and the brass pipe.

The blower was of radial blade, centrifugal type. It was driven by a 3- $\phi$ , 3 hp (440V, 4.5 A) induction motor. There were stepped pulleys connected by V-belts and the pulleys allowed two operating speeds for the blower. The maximum flow-rate of the blower under free operation was approximately 4 cfs. The inlet eye of the blower was fitted with an inlet duct assembly (Fig. 4.4) and a nozzle for measuring the flow-rate through the jet. The inlet duct



was made of  $1/16$ -inch M.S. plate. It was provided with an ordinary 2-inch gate valve in order to vary the flow-rate of air. Air from the blower was led to the settling chamber which was a 1-foot long, 6-inch nominal diameter G.I. pipe. The inside surface was carefully machined and polished by emery cloth. There was a flexible duct made of rubberized canvas in between the blower outlet and the settling chamber. The purpose of this duct was to arrest the vibration of the blower from being transmitted to the settling chamber. The air was then directed to the 2-feet long, 5-inch nominal diameter flow straightening section.

In this section there were packed 1-foot long,  $\frac{1}{2}$ -inch ID glass tubes (plate 4.4) of very small thickness (.018 inch) but of uniform bore. These tubes enabled the flow to become uniform and the vortices to die out which are formed by the action of a centrifugal blower. After the glass tubes there was a wire screen of fine mesh to make the flow uniform as far as possible.

The next part was the converging nozzle made of aluminium (Fig. 4.5a), the profile of which was a streamline obtained by a suitable rectilinear flow and source flow to fit the geometrical configuration. The streamlined surface had been chosen to allow minimum disturbance to flow.

Finally air was led to the detachable brass-pipe ( $1\frac{1}{4}$ - inch I.D. and  $11\frac{1}{2}$ - inch long) that produced the jet. There were two such brass-pipes. One was smooth (Fig. 4.6a) and the other had concentric stepped roughness inside (Fig. 4.6b). Both of these can be considered as extensions of the converging aluminium nozzle and had been machined from brass rods. They were fitted in turn to the nozzle to get different velocity profiles. The inside surface of the smooth nozzle was later covered with sands of two grain sizes ( $\epsilon = .0177$ " and  $\epsilon = .063$ " ) by means of adhesive to produce a pipe surface of different roughness. The grain size is defined on the basis of nominal sand dimension obtained from the seive numbers . The brass pipes were made tapered towards the opening such that the thickness at the exit was as small as practical by the available machining facilities in the machine shop. This was done so that the reduction of flow area for the induced flow can be kept at a minimum. The exit of the nozzle was located just at the entrance section of the mixing pipe.

#### 4.3. The Test Section

The test section was a 12-foot long, 3-inch nominal diameter (3.102-inch I.D) mild steel pipe. It was placed horizontally at a height of approximately 3-feet from the floor. The inside surface was cleaned with steel brush and the surface finished with emery cloth of different

grades. The test section was aligned ( § 4.5) carefully such that the exit of the jet was co-axial with the test section. The inlet to this test section was fitted with a streamlined bell- mouth (Fig. 4.5b) made of aluminium. In order to insert the pitot static tube vertically downward, twenty one  $3/8$  -inch diameter holes at different  $x/r_t$  values (First hole,  $x/r_t = 0.5$ , next six holes at an interval of  $x/r_t = 2$ , eighth to sixteenth holes at intervals of  $x/r_t = 4$ , last five holes at intervals of  $x/r_t = 8$  ) were made to measure velocity profiles. Static pressure tapings of  $\frac{1}{32}$  inch diameter were also made at each of these sections. Three more holes at  $x/r_t = 1, 3$  & 5 having a diameter of  $3/8$  - inch were also made in-line with twenty one holes for insertion of pitot tube in the vertical direction and for checking axial component of the possible back flow. When the velocities were measured at one section, all the other openings were kept closed with the help of M.S. plugs. The outlet from the test section led to an orificemeter with the help of which the total flow rate through the test section was determined.

#### 4.4 Flow Measuring Devices

Flow of air through the experimental set up was measured at two sections. These were 1) Measurement of air entering the blower with the help of an inlet nozzle

2) Measurement of the combined flow of air (jet and the induced flow) at the exit of the test section with the help of an orifice meter.

#### 4.4.1 The Inlet Nozzle

The inlet nozzle (Fig. 4.4), 2-inch throat diameter was made of aluminium. It was cast and later machined to have a streamlined profile. It was installed vertically with the mouth of the nozzle pointing upward. The nozzle was connected with the inlet duct of the blower. A pressure tapping (1/32 inch dia.) on this nozzle was made at the throat. The pressure tapping was connected to a draft gage (Ellison Company, USA) in order to measure the pressure depression in the nozzle for computation of flow rate. The nozzle was calibrated in place and the coefficient of discharge for different Reynolds number is shown in Fig. 4.10.

#### 4.4.2. The Orifice Meter

The orifice meter was installed at the end of the test section. It was made of 1/8-inch brass plate held concentrically between two flanges (Fig. 4.7). Two pieces of pipes were cut from the same run of mild steel pipe as the test section and fitted to the orifice meter on the up and down streams. There were two pressure tappings (3/32-inch diameter) at a distance of 1-dia. on the upstream and  $\frac{1}{2}$  dia. on the downstream of the orifice. The orifice plate along

with the pieces of pipes were calibrated before connecting with the test section.

The calibration of the orifice was done with the help of water (29) by direct weighing for the range of Reynolds number as would be expected in the actual test with air. The coefficient of discharge for different Reynolds number is plotted in figure 4.8.

#### 4.5 Alignment and Positioning of the Set Up

The different sections of the test rig were fabricated independently in different shops of the university. The sections were joined co-axially in the machine shop by flanges which were fastened by nuts and bolts. Dowel pins were provided at each junction for keeping proper alignments. The threads were made air-tight by employing Teflon tape and the flange connections were made air-tight by providing gaskets at each junction. These gaskets were of polythene paper and were covered with a thin layer of grease. The inlet duct of the blower was made air-tight by inserting 1/32-inch high pressure gasket with a thin layer of graphite.

The alignment was done in two phases. First the supports were bolted to the floor and levelled with spirit level. The final alignment was done by observing centering marks with the help of a telescope.

#### 4.6 Measurement of Velocity Profile and Static Pressure

The velocities were measured at twenty one stations along the test section to get the velocity profiles at these stations. A pitot static tube (1/16-inch O.D. hemispherical leading edge) was used with a draft gage using petroleum oil (specific gravity was 0.834) as the manometric liquid for this purpose. The pitot tube was held by a tube holder ( Fig. 4.9) made of brass. The tube holder along with the tube can be accurately traversed up and down within the test section with the help of an attachment (Fig. 4.9) fitted to a vertical stand provided with a vertical traversing mechanism. A vernier scale fitted with the traversing mechanism allowed it to give a minimum reading of 0.01 inch.

The static pressure tapings were made at twenty one  $x/D_t$  values along the test section as shown in figure 4.2. The pressure was transmitted through nipples held air-tight and perpendicular to the flow. The nipples were made of brass and machined carefully such that they just flush inside the surface of the test section (Fig. 4.3b). The outside parts of these were made tapered to ensure an air-tight fitting into the plastic tubes which were connected to the draft gage.

#### 4.7 Procedure of Measurement

The blower was first switched on and allowed to run for about fifteen minutes so that the transient characteristics died out. During the experiment the blower rpm was  $3873 \pm 2$  and that of the motor was  $1493 \pm 1$ . The flow was kept constant with the help of the controlling valve at the inlet duct and observing the draft gage at the inlet nozzle. All the draft gages used in the experiment employed petroleum oil having a specific gravity of 0.834 at a room temperature of about  $87^{\circ}\text{F}$ .

The height gage was levelled on a table placed near the test section. The pitot static tube was then put inside the mixing tube through one particular hole and alignment was done properly. During one set of reading all other holes were kept closed with the help of M.S. plugs and traversing was done at this station through a split-plug made of hardened rubber. In order to check the flow symmetry, the pitot tube was traversed from top surface to the bottom at a few stations; but the actual readings were taken from top surface to the centre line of the tube. The draft gages were carefully levelled with the help of spirit level. Since the pressure response of the draft gages dies out slowly, sufficient time was allowed before

taking the first reading on the draft gage. When one set of reading was complete at one station, the pitot tube was taken out, set at another station and the procedure was repeated. After one run of the experiment (at a particular Reynolds number and exit condition of the jet), the Reynolds number was changed with the help of the controlling valve. The experiments were conducted for three types of surface roughness of the nozzle. The first type was the smooth nozzle and experiments were conducted for four Reynolds number at nozzle exit. The inside surface of this nozzle was later covered with sand by glue to have a sand roughness. Two such surfaces were generated in turn by sands of two different grain sizes ( $\epsilon = 0.0177''$  and  $\epsilon = 0.063''$ ). For the nozzle with smaller grain size ( $\epsilon = .0177''$ ), experiments were conducted at three Reynolds number and for the other roughness ( $\epsilon = .063''$ ) at two Reynolds number. Another type of rough surface (discrete roughness) was tried by making concentric and square steps of  $\frac{1}{2}$  - inch pitch inside another brass rod (Fig. 4.6b). But due to high blockage and vibration observed during trial run readings were not taken with this nozzle.

Static pressures were taken at every tapping along the axial direction for each run of the experiment. The reading of the draft gage at orifice meter was also noted down for each set of experiment.



Temperatures at the exit of the jet and along the test section were measured with the help of a mercury thermometer. No appreciable temperature gradient was, however, detectable along the smooth pipe, except a few degrees ( maximum of  $5^{\circ}\text{F}$  under steady state operation) of temperature rise at the jet exit. The effect of this has been discussed in §6.3. Atmospheric temperatures ( dry bulb and wet bulb ) and pressure were also recorded for each run of experiment and proper care for their variations have been taken ( Appendix - C ).

#### 4.8 Error Analysis

In Appendix-C, the sources of error for different measurements are discussed quantitatively. The method proposed by Kline and McClintock (23) has been followed. The uncertainty in the measurement of mean velocities, static pressures and induced flow rates are determined. The errors obtained are found to be small enough to have any significant influences on the trends shown by different parameters.

CHAPTER - V  
RESULTS AND DISCUSSIONS

5.1 General

Mean velocities, pressure heads and flow-rates were measured and analysed to produce information regarding the flow and to determine the characteristics of the jet flow. Comments on the results of this investigation are given and the results are also compared with available informations in the literature.

5.2 Exit Conditions of the Jet

As mentioned in earlier chapters, the exit velocity profiles of jets were varied by changing the roughness of the inner surface of the nozzle. Experiments were performed at Reynolds numbers viz.,  $5.51 \times 10^4$ ,  $4.24 \times 10^4$ ,  $3.28 \times 10^4$  and  $2.39 \times 10^4$ . The velocity profiles at nozzle exit are plotted in figures 5.1, 5.2 & 5.3 and the values of the pertinent variables are shown in Table 5.1.

The displacement thickness is found to decrease with increase of Reynolds number for a particular type of nozzle. On the other hand, it ( $\delta^*$ ) increases with increase of roughness height for the same Reynolds number. This observation conforms with other authors (36). The radii of the potential core as is observed from Table 5.1, decrease

with increase of roughness height for the same Reynolds number. The shape factors indicate that the boundary layers at nozzle exit are turbulent in nature.

Table 5.1 Jet Exit Characteristics

Nozzle type	$Re_n \times 10^{-4}$	Total flow rate lb/s	$\delta^*_{o,n}$ inch	$\theta_{o,n}$ inch	H	$r_{pc}$ inch	$u_{c,n}$ ft/s
Smooth	2.39	.0263	.029	.0208	1.394	0.63	44.92
	3.28	.0362	.0275	.023	1.2	0.605	60.53
	4.24	.0439	.0235	.0209	1.124	0.58	73.55
	5.51	.0553	.0234	.0197	1.188	0.58	91.50
Nozzle Roughness $\epsilon/D_n = \frac{1}{70}$	2.39	.0263	.128	.0688	1.86	0.22	52.12
	3.28	.0362	.127	.070	1.81	0.20	71.66
	4.24	.0439	.124	.065	1.91	0.20	91.8
Nozzle Roughness $\epsilon/D_n = \frac{1}{20}$	2.39	.0263	.132	.079	1.674	0.05	67.56
	3.28	.0362	.131	.074	1.77	0.02	92.48

It is observed from the exit velocity profiles of jets as shown in figures 5.1, 5.2 & 5.3, that slight asymmetry is present in every profile. This error is probably due to a small misalignment of the set up, or it may be due to inaccuracy of the nozzle geometry. However, in the present work, this variation is neglected and measurements of the velocities were done for the top-half of the mixing pipe and results are based on these measurements.

### 5.3. Mean Velocity Profiles

The mean velocities along the downstream of the jet for each set of reading are shown in figures 5.4, 5.5 & 5.6. From these plots it is observed that initially the jet spreads inside the pipe for a few pipe diameters and then strikes the wall. The mean velocity readings away from the potential core are prone to errors due to possible recirculation and vorticity present at the outer region of the shear layer. By setting the pitot tube in the opposite direction of the flow draft gage readings were observed which was a clear indication of the presence of recirculation in the initial region of the jet.

The Craya-Curtet numbers for the experiments were found to vary within the range of 0.35-0.50. According to Becker, Hottel and Williams(6) if the value of CT is less than 0.8, recirculation will occur. Hence the observation of backward velocity indicating presence of recirculation conforms qualitatively with the observation of Becker et al as given above.

The mean velocity profiles in the duct flow region were checked at a few stations at the end of the test section. From the velocity profiles for the last two sections (at  $X=79.5$ ,  $X=87.5$ ) plotted in figures 5.4, 5.5 & 5.6, it appears that slight difference exists between the two consecutive stations, which indicates that the flow is still developing. For the present investigation the duct flow region

extends from  $X = 11.5$  to  $X = 87.5$  i.e., thirty-eight diameters ( $76 r_t$ ) only. From the literature on pipe flow it is found that development for turbulent cases occurs after 50 diameters from entrance, which agrees with the observation in the present situation.

#### 5.4 Axial Pressure Gradient

Axial pressure gradients of the smooth pipe for different Reynolds number and different types of jet exit condition are plotted in figure 5.7. All the curves show similar trends. The presence of negative pressure that is suction at the very beginning of the pipe ( $X = 1$ ) is an indication of induced mass flow due to the jet. The maximum pressure build-up occurs at axial distances of  $X = 8-10$ , which is just after the zone of attachment. This section of highest static pressure can be considered as the section of fully mixed flows. The maximum pressure rise has been compared with a theoretical model and the results are presented in Appendix - B. The results show that the experimentally determined values are close to those obtained theoretically. After the region of attachment the pressure shows a downward slope, which conforms to a pattern of simple turbulent flow through a smooth pipe. The pressure decrease in this zone is due to the

frictional resistance (Appendix- A) offered by the smooth pipe.

For the same Reynolds number at jet exit, the static pressures after the zone of attachment at every section shows an increasing trend with roughness height. This is due to the increased mass entrainment for the change of roughness height (Fig. 5.14).

### 5.5 Wall Shear Stress

The wall shear stresses were calculated for different sets of readings from the pressure gradient in the axial direction and the results are compared with Blasius equation for flow through smooth pipe (36). The shear stresses are found to increase with Reynolds number for all the sets. The variation of shear stress obtained by the two methods are within  $\pm 10\%$ .

### 5.6 Growth of the Jet and Attachment

The half-radius growth of the jets are shown in figures 5.8, 5.9, and 5.10. They show more or less similar increasing trends. Since the Reynolds number range was not much wide, the variation due to Reynolds number is not so prominent. The change of boundary layer at jet exit has

been found to have no appreciable effect on the region of attachment of the jet. For all sets of the experiment attachment took place between axial distances of  $X = 5.5$  and  $7.5$ . For smooth nozzle the half-radii at a particular location are distinctly different for different Reynolds number, and it is observed from the graph that higher is the Reynolds number higher will be the growth rate and consequently the attachment is likely to be at an earlier section at higher Reynolds number. This is, however, in conformity with the jet properties. On the other hand, for the other two types of nozzles, the points are more or less overlapping. A possible reason for this, is the bigger shear layer at the beginning which causes earlier mixing and thereby the differences due to Reynolds number on  $r_{\frac{1}{2}}$  are not so prominent.

### 5.7 Variation of Centre Line Velocity

The non-dimensional centre line velocities are plotted in figures 5.11, 5.12 and 5.13 for the initial regions of the flow. The constant velocity upto  $X = 1.5$  for different sets of nozzles reveals the existence of the potential core of the jet. After this constant velocity zone the curves fall sharply downward. At around  $X = 7.5 - 9.5$  the curvature decreases and show the beginning of duct-flow

region after attachment has taken place. The trends shown by the centre line velocities conform with the findings of other authors (11,19 & 21).

### 5.8 Induced Mass Flow Rate

The influences of Reynolds number as well as the velocity profile are distinctly observed on the rate of induced flow. For the same type of nozzle the mass induction increases with Reynolds number, which is in accordance with Sanger (33,34) and Mueller (26).

The influence of the boundary layer of the profile is also evident from fig. 5.14. At constant Reynolds number at nozzle exit, the induced mass flow rate increases with increase in shear layer of the jet at exit. This is due to better mixing of the secondary flow with the primary jet for increased thickness of the layer at the jet exit. Since the experiments could not be performed for a larger variation of flow rate, no correlation between the induced mass flow rate and Reynolds number was done. However, it is observed from figure 5.14 that for smooth nozzle the rate of increase of induced mass flow rate decreases with Reynolds number at nozzle exit.



### 5.9 Comparison of Excess Velocity Profiles

In figures 5.15, 5.16 & 5.17, the excess velocity profiles  $(u-u_s)/(u_c-u_s)$  vs.  $r/r_{\frac{1}{2}}$  are plotted. The matching with the empirical equation predicted by Hill (19) is the best for smooth nozzle. Whereas for other two types of nozzles, there are considerable scatter. Hill's equation is based on a large number of data collected for the developed velocity profiles of the jet from different authors. The range of Craya-Curtet number on which this equation is based is 0.31-1.3 and the range of the present investigation is within this limit. The scatter of the experimental points for the other two types of nozzles can be assigned to the boundary layer of the velocity profiles at jet exit.

## C H A P T E R - VI

### CONCLUSION

#### 6.1 General

In this chapter the findings and the limitations of the undertaken thesis are presented. Suggestions for future work are also given.

#### 6.2 Findings of the Present Work

The measurement of the flow development along the downstream of an axisymmetric jet revealed both well-known as well as not-so-known features. The study of mean velocity, jet growth, zone of attachment, pressure variation along the mixing duct and the rate of induced flow revealed some important and useful aspects of confined jet flow. These are enumerated below:

1. The zone of attachment is not a distinct point and is not found to vary with Reynolds number and with variation of boundary layer of velocity profile encountered in the experiment. The attachment takes place in between  $x/r_t = 5.5$  and  $x/r_t = 7.5$ .

2. The maximum pressure build-up occurs near the zone of attachment i.e., the region of fully mixed flow. The maximum pressure rise obtained experimentally can be predicted by the theoretical model shown in Appendix B.
3. The fully mixed section of the flow is followed by the duct flow region which is developing pipe flow.
4. A possible zone of recirculation exists in the initial region of the test section. Due to the presence of vortices, the flow pattern in this region is very much complicated and unstable.
5. The induced mass flow rate increases with increase of Reynolds number and increase of boundary layer at the jet exit. The maximum induced mass flow rate was found to be 21.95%, and it occurs at  $Re_n = 3.28 \times 10^4$  and  $\epsilon/Dn = 1/20$ .
6. The mean excess velocity profiles for the initial region fall on the same line by suitable choice of the other coordinate axis (e.g.,  $r/r_{\frac{1}{2}}$ ) for different Craya-Curtet numbers.

### 6.3 Limitations of the Study

The main constraint in this study was the low capacity of the blower and consequently the low Reynolds number of the jet. If the Reynolds number could be increased, preferably to the order of  $10^5$ , more data could be generated for each roughness and initial velocity profile of the jet could be varied to a larger extent.

Since the blower was used to supply air for the jet, there was a slight increase in temperature of the jet flow. In fact, for this reason and not to aggravate the situation the flow was not increased by increasing the rpm of the blower. The temperature rise mainly affects the Reynolds number. Since the mean velocities were measured and the variations were not much (less than .05% ), the effect of temperature was ignored.

The length of the test section was taken to be 11-ft i.e.,  $x/D_t = 44$ . The velocity profile though very near to developed was not fully developed and thus a definite conclusion could not be given about the flow development.

### 6.4 Extensions of the Present Work

The study of induced flow development along the downstream of an axisymmetric jet issuing axially into a smooth pipe has been undertaken and the results have been presented in this thesis. A basic experimental facility

has been developed for this purpose. But due to some limitations of the study ( §6.3), a limited amount of data have been generated. As such with some modifications of the experimental facility more data can be obtained to analyse the situation for better understanding of the flow. Hence as an extension of the present work, the following suggestions may be made for further work in this field.

1. The blower can be replaced by an axial flow fan and experiments may be conducted at higher Reynolds numbers.
2. The type of roughness of the jet nozzle can be varied over a wider range and any correlation, if any, between the exit velocity profile and the corresponding flow development may be established.
3. The ratio of mixing duct diameter and that of the nozzle can be varied and experiments may be done for different aspect ratios.
4. The length of the test section may be made much larger (about sixty diameters) in order to get the developed flow on the downstream side.

5. The recirculation in the initial region can be studied.
6. The location of the exit plane of jet nozzle can be varied with respect to the inlet section of the mixing pipe and the flow characteristics in the downstream can be studied.
7. For all the flow configurations mentioned above, the turbulence parameters can be measured by proper instrumentation.

APPENDIX - A

DETERMINATION OF WALL SHEAR STRESSES

After the jet strikes the wall, the flow is a simple pipe flow in the turbulent region. So the investigation has not been made in this region except for the static pressure gradient in axial direction. The static pressure as is seen from Fig. 5.7 decreases linearly with axial distance as has already been mentioned in §5.5.

The wall shear stress for smooth pipe is obtained by two independent methods and comparison is made.

The first method employs determining the wall shear stress of the smooth duct by the formula described by Schlichting (36).

$$\tau_w = 1/8 f \rho \bar{U}_t^2 \quad \dots \quad (A.1)$$

where  $f$  is the resistance coefficient, which is determined from the formula by Blasius (36) for smooth duct.

$$f = 0.3164 Re_t^{-1/4} \quad \dots \quad (A.2)$$

From equations (A.1) and (A.2), it is obtained

$$\tau_w = 0.03955 \rho \bar{U}_t^2 Re_t^{-1/4} \quad \dots \quad (A.3)$$

where  $\rho$  is in slug/ft<sup>3</sup>. The values obtained for different sets of reading are shown in table A.1.

The second method is the determination of wall shear stress from axial pressure gradient of the pipe. If the wall shear stress is assumed to be uniform throughout the perimeter of the duct, then a simple force balance provides,

$$\tau_w = \left( \frac{dp}{dx} \right)_w \frac{D_t}{4} \quad \dots \quad (A.4)$$

where  $dp/dx$  is the pressure gradient assessed from the wall static pressures measured by the wall tappings. The values obtained by this method are also shown in Table A.1.

Table A.1 Wall Shear Stresses Calculated By Different Methods.

Type of Nozzle	$Re_t \times 10^{-4}$	$\tau_w$ from eqn. (A.3) $lb_f/ft^2$	$\tau_w$ from eqn. (A.4) $lb_f/ft^2$
Smooth	1.15	.000498	.000472
	1.63	.000907	.000671
	2.01	.00132	.00124
	2.59	.00205	.00220
Nozzle Roughness	1.16	.00050	.00053
	1.65	.00093	.000753
	$\epsilon/D_n = 1/70$ 2.03	.00132	.0012
Nozzle Roughness	1.17	.00051	.00045
	$\epsilon/D_n = 1/20$ 1.80	.0011	.00096



## APPENDIX - B

### DETERMINATION OF MAXIMUM PRESSURE RISE

In order to predict the maximum pressure rise for the type of induced flow as in the present case, the simple theoretical model similar to the one by Hill, B.J.(20) is presented here. The essential assumptions for this model are:

1. The maximum pressure in the mixing duct corresponds to complete mixing of the primary and secondary streams;
2. The primary, secondary and fully mixed flow are each of uniform velocity across the respective cross-sectional areas;
3. The pressure is uniform in the inlet plane and the plane of maximum pressure rise;
4. The density change due to slight change in pressure is neglected;
5. The wall friction force is negligible in comparison with the pressure force.

These assumptions approximately hold good for the flow situation in the present investigation. By taking a control volume between the inlet section and the section of maximum pressure rise, the force balance gives the following equation:

$$(p_2 - p_1) \rho A_t = \dot{m}_t \bar{u}_t - \dot{m}_n \bar{u}_n - \dot{m}_s \bar{u}_s \quad \dots \quad (B.1)$$

where,

$\dot{m}_n$  = mass flow rate through the nozzle

$\dot{m}_t$  = mass flow rate through the duct at the section of maximum pressure rise

$\dot{m}_s$  = secondary mass flow rate =  $\dot{m}_t - \dot{m}_n$  ... (B.2)

$\bar{u}$  = area mean velocities

$P_1, P_2$  = static pressures at the inlet section and section of maximum pressure.

Now,  $\bar{u}_n = \dot{m}_n / (\rho A_n)$  ... (B.3)

$\bar{u}_t = \dot{m}_t / (\rho A_t)$  ... (B.4)

The thickness of the jet nozzle reduces the flow area of the secondary stream. Hence, to calculate the flow rate of this stream the area is corrected by introducing the 'thickness correction factor' C. So

$\bar{u}_s = \dot{m}_s / (A_t - CA_n) \rho$  ... (B.5)

By substituting eqns. (B.2), (B.3), (B.4) and (B.5) in equation (B.1) and introducing  $C' = A_n/A_t$  the expression for maximum pressure rise ( $\Delta P$ ) becomes,

$$\Delta P = \frac{1}{\rho A_t A_n} \left[ (\dot{m}_n^2 - C' \dot{m}_t^2) + \frac{C'}{1 - CC'} (\dot{m}_t - \dot{m}_n)^2 \right] \dots (B.6)$$

For one set of reading (Nozzle roughness,  $\epsilon/D_n = 1/70$  and  $Re_n = 3.28 \times 10^4$ ) the following values were obtained:

$$\dot{m}_n = .0362 \text{ lb/s}, \dot{m}_t = .04265 \text{ lb/s}$$

$$A_n = .00852 \text{ ft}^2 \quad A_t = .05241 \text{ ft}^2 \quad C' = A_n/A_t = .1626$$

$$C = 1 + \frac{(1.344)^2 - (1.25)^2}{(1.25)^2} = 1.156 \quad (\text{Fig. 4.6a})$$

$$\rho = .0719 \text{ lb/ft}^3$$

$$\Delta P_{\text{exp.}} = .905 \text{ lb}_f/\text{ft}^2$$

From eqn. (B.6),

$$\Delta P_{\text{theor.}} = .989 \text{ lb}_f/\text{ft}^2$$

$$\frac{\Delta P_{\text{theoretical}}}{\Delta P_{\text{experimental}}} = 1.09$$

The comparison of the maximum pressure rise for all the sets are shown below.

Table B.1 Comparison Of Maximum Pressure Rise With Theoretical Model.

Type of Nozzle	$Re_n \times 10^{-4}$	$\Delta P_{\text{experimental}}$ $\text{lb}_f/\text{ft}^2$	$\Delta P_{\text{theoretical}}$ $\text{lb}_f/\text{ft}^2$	$\frac{\Delta P_{\text{theor.}}}{\Delta P_{\text{exp.}}}$
	2.39	0.424	0.539	1.271
	3.28	0.853	1.011	1.1845
Smooth	4.24	1.420	1.473	1.037
	5.51	2.236	2.315	1.036
Nozzle Roughness	2.39	0.481	0.528	1.098
$\epsilon/D_n = 1/70$	3.28	0.905	0.989	1.09
	4.24	1.518	1.450	0.955
Nozzle Roughness	2.39	0.545	0.596	0.966
$\epsilon/D_n = 1/20$	3.28	1.009	0.974	0.965

APPENDIX - C

UNCERTAINTY ANALYSIS FOR MEAN QUANTITY MEASUREMENTS

In the present investigation, measurements were taken with great care to minimise the possible sources of error. But the inherent limitations of the draft gages and the measuring instruments, the atmospheric changes and the probe settings introduced some errors in the process of measurements. Uncertainties thus crept into the measurements of velocity and pressure are analysed by the method suggested by Kline and McClintock (23).

If a result  $R$  be a function of  $n$  independent variables  $v_1, v_2, \dots, v_n$

$$R = R ( v_1, v_2, \dots, v_n ) \quad \dots \quad (C.1)$$

For small variations in the variables, the relation can be expressed in linear form as

$$R = \frac{\partial R}{\partial v_1} \delta v_1 + \frac{\partial R}{\partial v_2} \delta v_2 + \dots + \frac{\partial R}{\partial v_n} \delta v_n \quad \dots (C.2)$$

The uncertainties in the variables  $v_n$  are represented completely by an uncertainty distribution but can be adequately described by uncertainty intervals  $U_{v_n}$ .

If  $U_R$  is the uncertainty involved with the result, then

$$U_R = \left[ \left( \frac{\partial R}{\partial v_1} U_{v_1} \right)^2 + \left( \frac{\partial R}{\partial v_2} U_{v_2} \right)^2 + \dots + \left( \frac{\partial R}{\partial v_n} U_{v_n} \right)^2 \right]^{\frac{1}{2}} \dots (C.3)$$

This equation for the calculation of uncertainty has been used in the following analyses.

### C.1 Uncertainty in Mean Velocity Measurements

When air was flowing with a velocity  $u$  (ft/s) and a pitot-static was placed parallel to the flow, the velocity was calculated from the dynamic head  $hw$  (ft) of water recorded by the draft gage reading from the relation

$$u = \sqrt{\frac{2g \quad hw \quad \gamma_w}{\gamma_a}} \dots (C-1.1)$$

where  $\gamma_w$  and  $\gamma_a$  were the specific weights of water and air respectively. The scale readings of draft gages were for a pressure of 29.92 inches of Hg and for dry air at 70°F. So,

$$u = 66.75 \sqrt{hw} \dots (C-1.2)$$

where  $hw$  was draft gage reading in inch under the standard conditions mentioned above. But for the present case, the temperature, pressure and humidity were different and proper correction factors were applied. Hence it was not necessary to calculate the uncertainty involved due to these changes. The only factor that caused the uncertainty was the meniscus

reading,  $hw$ . The change of density of oil used in draft gages due to fluctuation of laboratory temperature (maximum of  $\pm 2^{\circ}\text{F}$ ) was found to be negligibly small in comparison with the meniscus fluctuation and had negligible effect on the final reading. Specific gravity of oil was .834.

If the sensing point of the pitot-static had a misalignment of  $\theta$  from the direction of flow due to adjustment error, then the measured value would be

$$u = C \sqrt{hw} \cos \theta \quad \dots \quad (\text{C-1.3})$$

$$\text{where } C = 66.75 \times C_1 \times C_2 \quad \dots \quad (\text{C-1.4})$$

$C_1$  and  $C_2$  being the correction factors for temperature-pressure and humidity respectively.

From eqn. (C.3), the uncertainty in velocity measurement can be expressed as

$$U_u = \left[ \left( \frac{\partial u}{\partial hw} U_{hw} \right)^2 + \left( \frac{\partial u}{\partial \theta} U_{\theta} \right)^2 \right]^{\frac{1}{2}} \quad \dots \quad (\text{C-1.5})$$

where  $U_{hw}$  and  $U_{\theta}$  are uncertainties associated with draft-gage reading and alignment of the probe with flow direction.

To get the uncertainties involved in the different variables the respective partial derivatives are now found out.

$$u = C \sqrt{hw} \cos \theta \quad \dots \quad (C-1.3)$$

$$\frac{\partial u}{\partial hw} = \frac{C}{2} \frac{1}{\sqrt{hw}} \cos \theta \quad \dots \quad (C-1.6)$$

$$\frac{\partial u}{\partial \theta} = -C \sqrt{hw} \sin \theta \quad \dots \quad (C-1.7)$$

Combining these equations with eqn. (C-1.5),

$$U_u = \frac{C}{2} \cos \theta \left[ \frac{1}{hw} U_{hw}^2 + 4 hw U_\theta^2 \tan^2 \theta \right]^{\frac{1}{2}} \quad \dots \quad (C-1.8)$$

From equations (C-1.3) and (C-1.8), the equation for uncertainty in velocity measurement takes the form

$$\frac{U_u}{u} = \frac{1}{2} \left[ \frac{U_{hw}^2}{hw^2} + 4 U_\theta^2 \tan^2 \theta \right]^{\frac{1}{2}} \quad \dots \quad (C-1.9)$$

Now during an experimental run, the following conditions were observed.

$$hw = .3 \pm .005 \text{ inch of water}$$

$$\theta = 0^\circ \pm 3^\circ$$

The corresponding uncertainty in the velocity measurement from the equation is computed to be  $U_u/u = 0.0169$  or 1.69%.

## C-2 Uncertainty in Static Pressure Measurement

The wall static pressures measured from the wall tappings were the gage pressures below and above atmospheric pressure. If  $p$  be the absolute static pressure and  $p_a$  be the atmospheric pressure, then the recorded pressure would be

$$p_r = p_a - p \quad \dots \quad (C-2.1)$$

and the absolute static pressure

$$p = p_a - p_r \quad \dots \quad (C-2.2)$$

The recorded pressure is nothing but  $\gamma_w hw$ , so that

$$p = p_a - \gamma_w hw \quad \dots \quad (C-2.3)$$

Hence the uncertainty in wall static pressure measurement was

$$U_p = \left[ \left( \frac{\partial p}{\partial p_a} U_{p_a} \right)^2 + \left( \frac{\partial p}{\partial \gamma_w} U_{\gamma_w} \right)^2 + \left( \frac{\partial p}{\partial hw} U_{hw} \right)^2 \right]^{1/2} \quad (C-2.4)$$

$$\partial p / \partial p_a = 1, \quad \partial p / \partial \gamma_w = -hw \quad \text{and} \quad \partial p / \partial hw = -\gamma_w \quad (C-2.5)$$

Substituting (C-2.5) in (C-2.4)

$$U_p = \left[ U_{p_a}^2 + hw^2 U_{\gamma_w}^2 + \gamma_w^2 U_{hw}^2 \right]^{1/2} \quad \dots \quad (C-2.6)$$

For an experimental run,

$$p = 2102.4 \text{ psf}, \quad U_{p_a} = 0, \quad \text{for a short interval}$$

$$hw = .091 \pm .001 \text{ inch of water}, \quad \gamma_w = 62.241 \pm .032 \text{ lb/ft}^3$$

The corresponding uncertainty from equation is

$$\frac{U_p}{p} = 4.935 \times 10^{-6} \text{ i.e., } .0005\%$$



C-3 Uncertainty in Determination of Induced Flow Rate

The induced flow rate through the mixing duct was calculated from the difference between the total flow rate through the orifice and that through the inlet nozzle. Since the air coming out of the blower was at a temperature of about 5°F higher than that of the ambient secondary air, the induced flow rate was calculated in mass unit after taking proper care for the change of density. The small variation of pressure has negligible effect on the flow rates. If  $\dot{m}$  is the induced flow rate,  $\dot{m}_t$ , the total flow rate through orifice and  $\dot{m}_n$ , the flow rate through the inlet nozzle, then

$$\dot{m} = \dot{m}_t - \dot{m}_n \quad \dots \quad (C-3.1)$$

$$\dot{m}_t = k_1 Cd_1 \sqrt{h_1} \quad \dots \quad (C-3.2)$$

$$\dot{m}_n = k_2 Cd_2 \sqrt{h_2} \quad \dots \quad (C-3.3)$$

where  $k_1$  and  $k_2$  are constants obtained from geometry of the devices and  $Cd_1$  and  $Cd_2$  are the coefficients of discharge of the orifice plate and of the nozzle respectively. Therefore, the uncertainty in the determination of induced mass flow rate is

$$U_{\dot{m}} = \left[ \left( \frac{\partial \dot{m}}{\partial \dot{m}_t} U_{\dot{m}_t} \right)^2 + \left( \frac{\partial \dot{m}}{\partial \dot{m}_n} U_{\dot{m}_n} \right)^2 \right]^{\frac{1}{2}} \quad \dots (C-3.4)$$

where  $U_{\dot{m}_t}$  and  $U_{\dot{m}_n}$  are the uncertainties associated with  $\dot{m}_t$  and  $\dot{m}_n$ .

By taking partial derivatives of eqn. (C-3.1)

$$\partial \dot{m} / \partial \dot{m}_t = 1, \quad \partial \dot{m} / \partial \dot{m}_n = -1 \quad \dots \quad (\text{C-3.5})$$

Substituting eqn. (C-3.5) in (C-3.4)

$$U_{\dot{m}} = [ U_{\dot{m}_t}^2 + U_{\dot{m}_n}^2 ]^{\frac{1}{2}} \quad \dots \quad (\text{C-3.6})$$

$$\dot{m}_t = k_1 C d_1 \sqrt{h_1} \quad \dots \quad (\text{C-3.2})$$

$$U_{\dot{m}_t} = [ ( \frac{\partial \dot{m}_t}{\partial C d_1} U_{C d_1} )^2 + ( \frac{\partial \dot{m}_t}{\partial h_1} U_{h_1} )^2 ]^{\frac{1}{2}} \quad (\text{C-3.7})$$

$$\partial \dot{m}_t / \partial C d_1 = k_1 \sqrt{h_1} \quad \dots \quad (\text{C-3.8})$$

$$\partial \dot{m}_t / \partial h_1 = k_1 C d_1 / 2 \sqrt{h_1} \quad \dots \quad (\text{C-3.9})$$

Substituting (C-3.8) and (C-3.9) in (C-3.7) and combining with (C-3.2)

$$\frac{U_{\dot{m}_t}}{\dot{m}_t} = [ ( \frac{U_{C d_1}}{C d_1} )^2 + \frac{1}{4} ( \frac{U_{h_1}}{h_1} )^2 ]^{\frac{1}{2}} \quad \dots \quad (\text{C-3.10})$$

Similarly, for the nozzle

$$\frac{U_{\dot{m}_n}}{\dot{m}_n} = [ ( \frac{U_{C d_2}}{C d_2} )^2 + \frac{1}{4} ( \frac{U_{h_2}}{h_2} )^2 ]^{\frac{1}{2}} \quad \dots \quad (\text{C-3.11})$$

Now, for an experimental run ( $Re_n = 3.28 \times 10^4$ , Nozzle roughness  $\epsilon/D_n = 1/20$ )

$$Cd_1 = 0.635 \pm .002, \quad h_1 = 0.33 \pm .005 \text{ inch of water}$$

$$U_{\dot{m}_t} / \dot{m}_t = .008204 \quad \dots \quad (C-3.12)$$

$$Cd_2 = .879 \pm .002, \quad h_2 = 0.15 \pm .001 \text{ inch of water}$$

$$U_{\dot{m}_n} / \dot{m}_n = .00403 \quad \dots \quad (C-3.13)$$

For this set,

$$\dot{m}_t = .0441 \text{ lb/s}, \quad \dot{m}_n = .0362 \text{ lb/s}$$

Hence substituting in eqn. (C-3.6) and dividing by

$\dot{m} = .0079 \text{ lb/s}$ , the uncertainty in induced mass flow rate is

$$\frac{U_{\dot{m}}}{\dot{m}} = 0.0494 \text{ i.e., } 4.94\%$$

## REFERENCES

1. Antonia, R.A., and Bilger, R.W., " An experimental investigation of an axisymmetric jet in a co-flowing air stream", J. Fluid Mechanics, Vol. 61, part 4, p. 805 - 822, 1973.
2. Azim, M.A., "Numerical computation for velocity and temperature within the axisymmetric turbulent jets in moving surrounding", M.Sc.(Engg.) Thesis, Deptt. of Mechanical Engineering, Bangladesh University of Engineering and Technology, Dhaka, December 1984.
3. Barchilon, M., and Curtet, R., "Some details of the structure of an axisymmetric confined jet with backflow", Transactions of ASME, J. Basic Engineering, p. 777-787, December 1964.
4. Beavers, G.B., and Theodore, A.W., "Vortex growth in jets", J. Fluid Mechanics, vol. 44, part 1, p.97-112, 1970.
5. Becker, H.A. and Brown, A.P.G., "Response of Pitot probes in turbulent streams", J. Fluid Mechanics, vol. 62, part 1, p. 85-114, 1974.
6. Becker, H.A., Hottel, H.C., and Williams, G.C., "Mixing and flow in ducted turbulent jets", Ninth International Symposium on Combustion, Academic Press, New York, N.Y., p. 7-20, 1965.
7. Bogslawski, L., and Popiel, Cz.O., "Flow structure of the free round turbulent jet in the initial region", J. Fluid Mechanics, vol. 90, part 3, p. 531-539, 1979.
8. Bradshaw, P., "The effect of initial conditions on the development of a free shear layer", J. Fluid Mechanics, vol. 26, part 2, p. 225-236, 1966.

9. Chassing, P., and Minh, H.Ha, "Orderly structure of jet turbulence", J. Fluid Mechanics, vol 48, part 3, p. 547-591, 1977.
10. Chu, W.T., "Velocity profile in the half-jet mixing region of turbulent jets", AIAA Journal , vol. 3, No. 4, p. 789-790, April 1965.
11. Curtet, R., and Ricou, F.P., "On the tendency to self-preservation in axisymmetric ducted jets", Transactions of ASME, J. Basic Engineering, p. 765-776, December 1964.
12. Evertt, K.W., and Robins, A.G., "The development and structure of turbulent plane jets", J. Fluid Mechanics, vol. 88, part 3, p. 563-568, 1978.
13. Exley, J.T., and Brighton, J.A., "Flow separation and reattachment in confined jet mixing", Transactions of ASME, p. 210-220, March 1967.
14. Gurevich, M.I., Theory of Jets in Ideal Fluids, Academic Press, N.Y. , and London, 1965.
15. Habib, M.A., and Whitelaw, J.H., "Velocity characteristics of a confined coaxial jet", Transactions of ASME, vol. 101, p. 521-529, December 1979.
16. Hall, L.C., "An apparatus illustrating the momentum principle", International J. Mechanical Engineering Education, vol. 5, No. 3, p. 229-237, July 1977.
17. Hasan, M.A.Z., and Hussain, A.K.M.F., "The self-excited axisymmetric jet", J. Fluid Mechanics, vol. 115, p. 59-89, 1982.
18. Heskestad, G., "Hot-wire measurements in a radial turbulent jet", ASME J. International Flow, G. Sovran, ed., Elsevier, p. 170-201, 1967.

19. Hill, B.J., "Two-dimensional analysis of flow in jet pumps", ASCE, J. Hydraulics Division, vol. 99, No. HY7, p. 1009-1026, July 1973.
20. Hill, B.J., "An experiment involving the construction of a theoretical model", Bulletin of Mechanical Engineering Education, vol. 9, p. 137-140, May 1970.
21. Hill, P.G., "Incompressible jet mixing in converging-diverging axisymmetric ducts", Transactions of ASME, J. Basic Engineering, p. 210-220, March 1967.
22. Hill, P.G., "Turbulent jets in ducted streams", J. Fluid Mechanics, vol. 22, part 1, p. 161-186, 1965.
23. Kline, S.J., and McClintock, F.A., "Describing uncertainties in single -sample experiments", Mechanical Engineering, vol. 75, No. 1, p.3-8, 1958.
24. Kotsovinos, N.E., "A note on the conservation of axial momentum of a turbulent jet", J. Fluid Mechanics, vol. 87, part 1, p. 55-63, 1978.
25. Lau, J.C., "Effects of Mach number and temperature on mean flow and turbulence characteristics in round jets", J. Fluid Mechanics, vol. 105, p. 193-218, 1981.
26. Mikhail, S., "Mixing of coaxial streams inside a closed conduit", J. Mechanical Engineering Science, vol. 2, p. 59-68, 1960.
27. Mueller, N.H.G., "Water jet pumps", ASCE, J. Hydraulics Division, HY3, p. 83-113, May 1964.

28. Newman, B.G., "The prediction of turbulent jets and wall jets", Canadian Aeronautics and Space Journal, vol.15, No. 8, p. 287-305.
29. Ower, E., and Pankhurst, R.C., The Measurement of Air Flow, 5th edition, Pergamon Press.
30. Rankine, J.M., "On the mathematical theory of combined streams", Royal Soc., London, England, 1870. (Referenced in Mueller, N.H.G., "Water jet pumps" ASCE, J. Hydraulics Division, HY 3, p. 83-113, May 1964).
31. Razinsky, E., and Brighton, J.A., "Confined jet mixing for non-separating conditions", Transactions of ASME, J. Basic Engineering. p. 333-349, September 1971.
32. Roshko, A., "Structure of turbulent shear flows ; A new look", AIAA Journal, vol. 14, No. 10, p.1349-1357 October 1976.
33. Sanger, N.L., "Noncavitating performance of two low-area-ratio water jet pumps having throat lengths of 7.25 diameters", National Aeronautics and Space Administration, TN D-4445, 1968.
34. Sanger, N.L., " Noncavitating and cavitating performance of two low- area ratio water jet pumps with throat lengths of 5.66 diameters", National Aeronautics and Space Administration, TN D-4759,1968.
35. Saph, V., and Schoder, E.H., "An experimental study of the resistance to the flow of water in pipes", Transactions of ASCE, vol. 51, p. 944, 1903.
36. Schlichting, H., Boundary Layer Theory, 6th edition, McGraw Hill Series in Mechanical Engineering, 1968.

37. Stanton. T.E., and Pannel, J.R., "Similarity of motion in relation of the surface friction of fluids", Phil. Transactions, Royal Society, 1914, A214,199.
38. Taylor, G.I., "Some early ideas about turbulence", J. Fluid Mechanics, vol. 41, part 1, p. 3-11, 1970.
39. Thomson, J., "On a jet pump or apparatus for drawing up water by the power of a jet", Report, British Assn., London, p. 130, 1852 ( Referenced in Mueller, N.H.G, "Water jet pumps", ASCE, J. Hydraulics division,HY3, p. 83-113, May 1964 ).
40. Townsend, A.A., The Structure of Turbulent Shear Flow, Cambridge University Press, 1956.
41. Wagnanski, I., and Fiedler, H., "Some measurements in the self- preserving jets", J. Fluid Mechanics, vol. 38, series E, p. 417-424, June 1966.



LIST OF FIGURES

<u>FIG.</u>		<u>PAGE</u>
2.1	Coordinate System & Flow Regions	61
4.1	Schematic Diagram of Experimental Set Up	62
4.2	Location of Static Pressure Holes	63
4.3 a,b	Details of Plugs and Nipples	64
4.4	The Inlet Duct Assembly	65
4.5a	The Converging Nozzle	66
4.5b	The Bell-Mouth	66
4.6a,b	Detachable Brass Nozzles	67
4.7	Details of Orifice Section	68
4.8	Calibration Curve for Orifice	69
4.9	Pitot-Tube and Attachments	70
4.10	Calibration Curve for Inlet Nozzle	71
5.1-5.3	Mean Velocity Profiles at Nozzle Exit	72
5.4-5.6	Mean Velocity Profiles along the Duct	77
5.7	Static Pressure Distribution	82
5.8-5.10	Variation of Half-radius with Axial Distance	83
5.11-5.13	Centre Line Velocity Distribution	86
5.14	Rate of Induced Mass Flow	89
5.15-5.17	Comparison of Excess Velocity Profiles	90

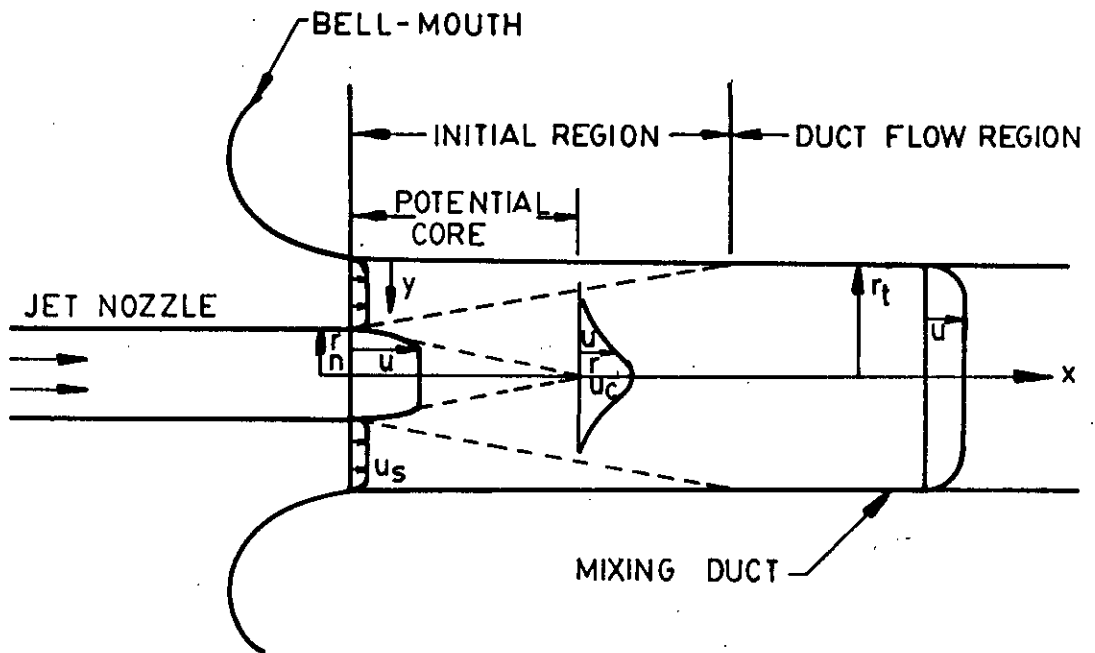


FIG. 2-1. COORDINATE SYSTEM &amp; FLOW REGIONS

- 1 MOTOR
- 2 BLOWER
- 3 INLET DUCT
- 4 FLEXIBLE DUCT
- 5 SETTLING CHAMBER
- 6 FLOW STRAIGHTENING SECTION
- 7 WIRE MESH
- 8 CONVERGING NOZZLE
- 9 REPLACEABLE BRASS PIPE
- 10 BELL MOUTH
- 11 MIXING DUCT/TEST SECTION
- 12 ORIFICE METER
- 13 SUPPORTS

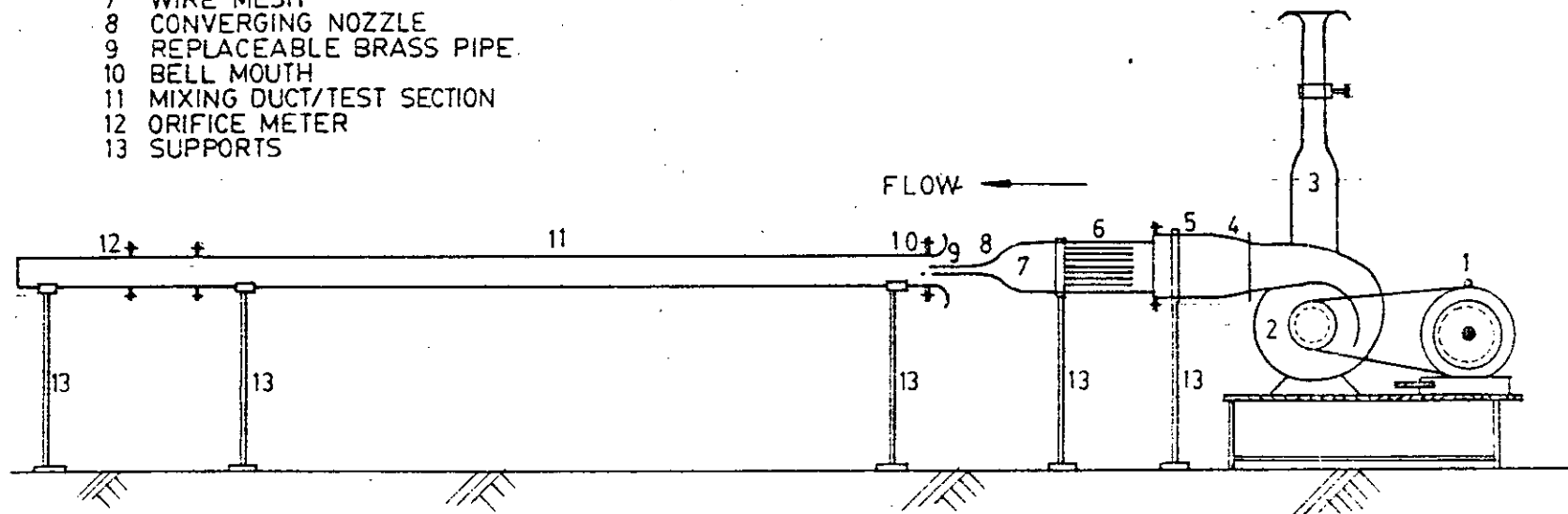


FIG. 4-1 SCHEMATIC DIAGRAM OF EXPERIMENTAL SET-UP

66096

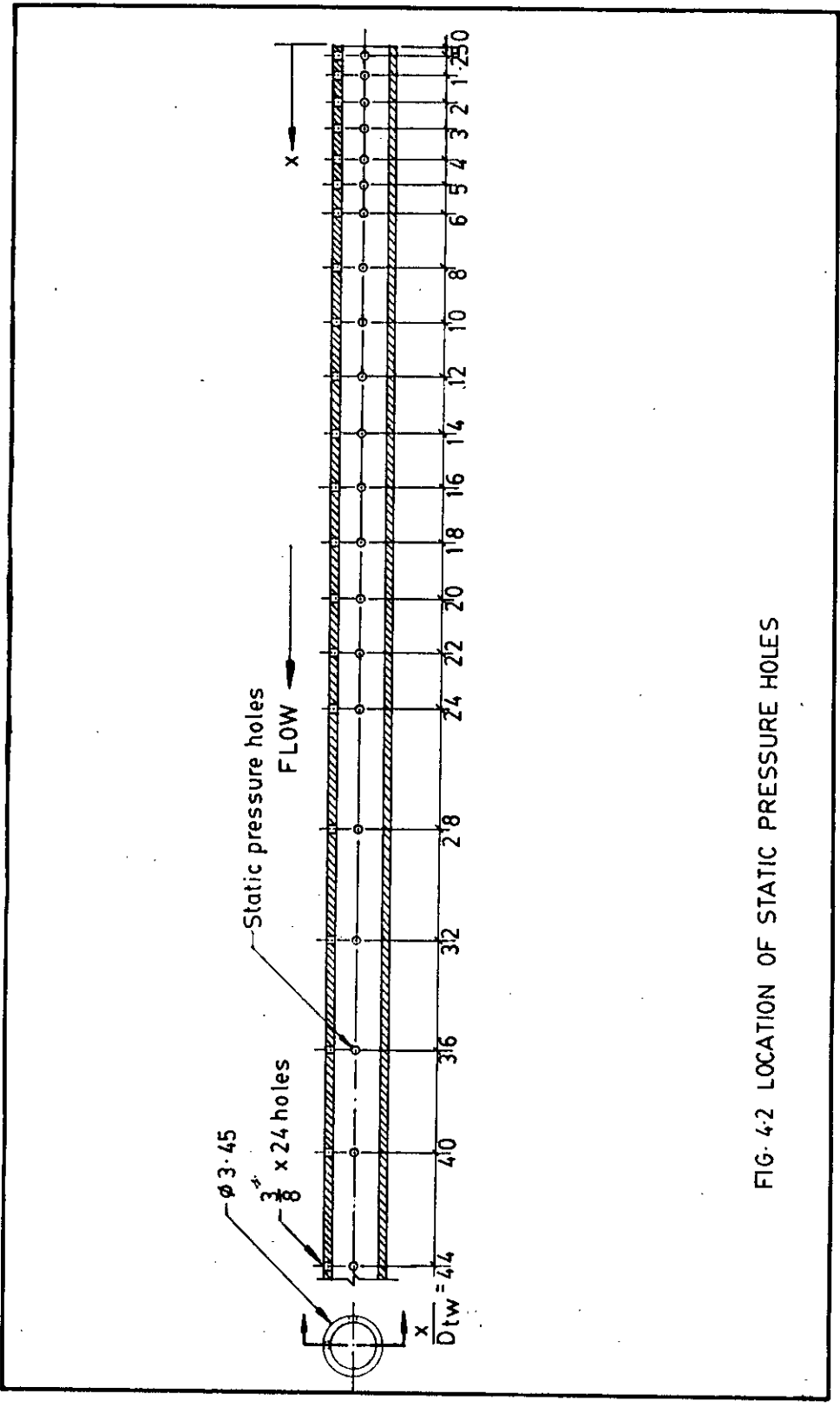


FIG 4-2 LOCATION OF STATIC PRESSURE HOLES



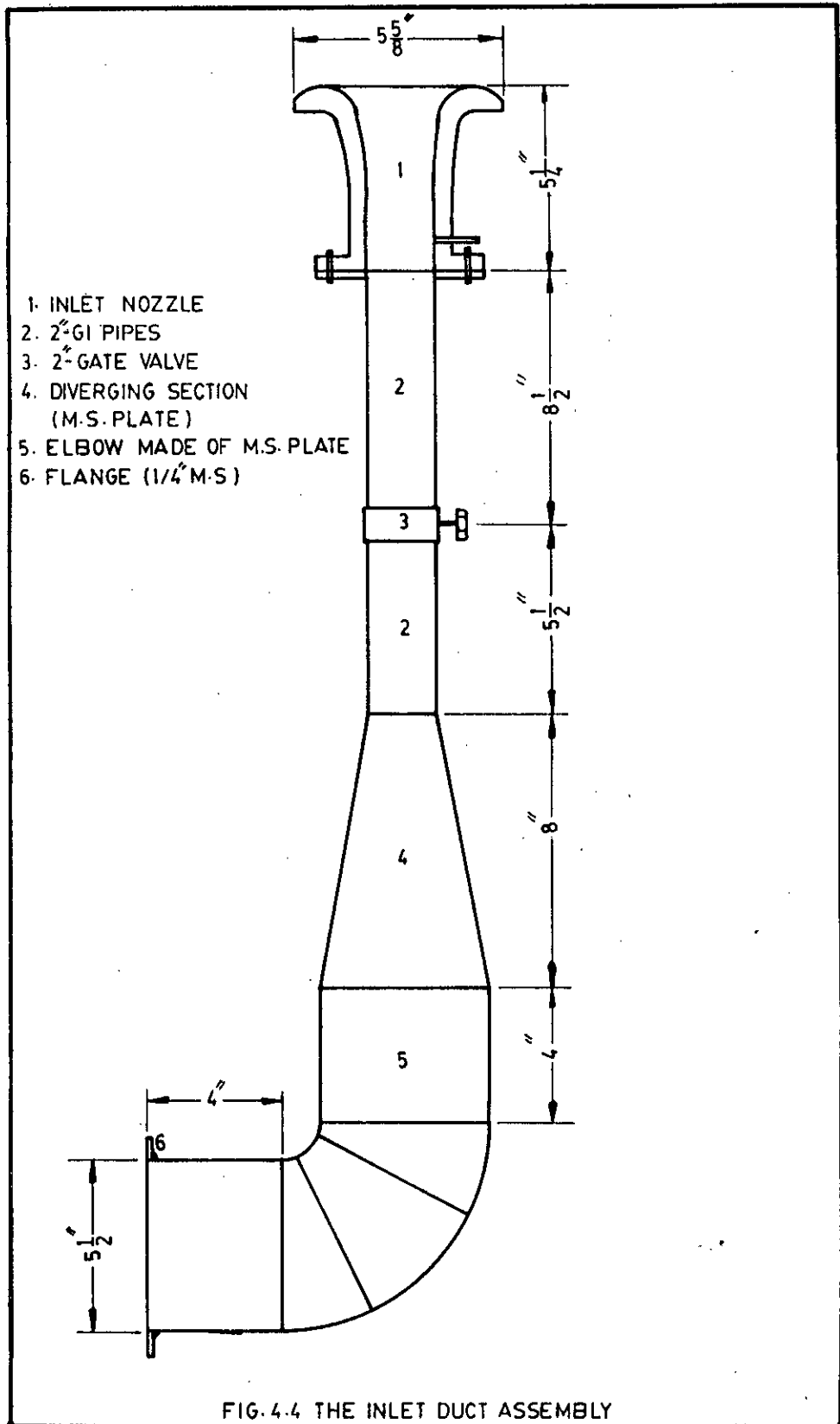


FIG. 4.4 THE INLET DUCT ASSEMBLY

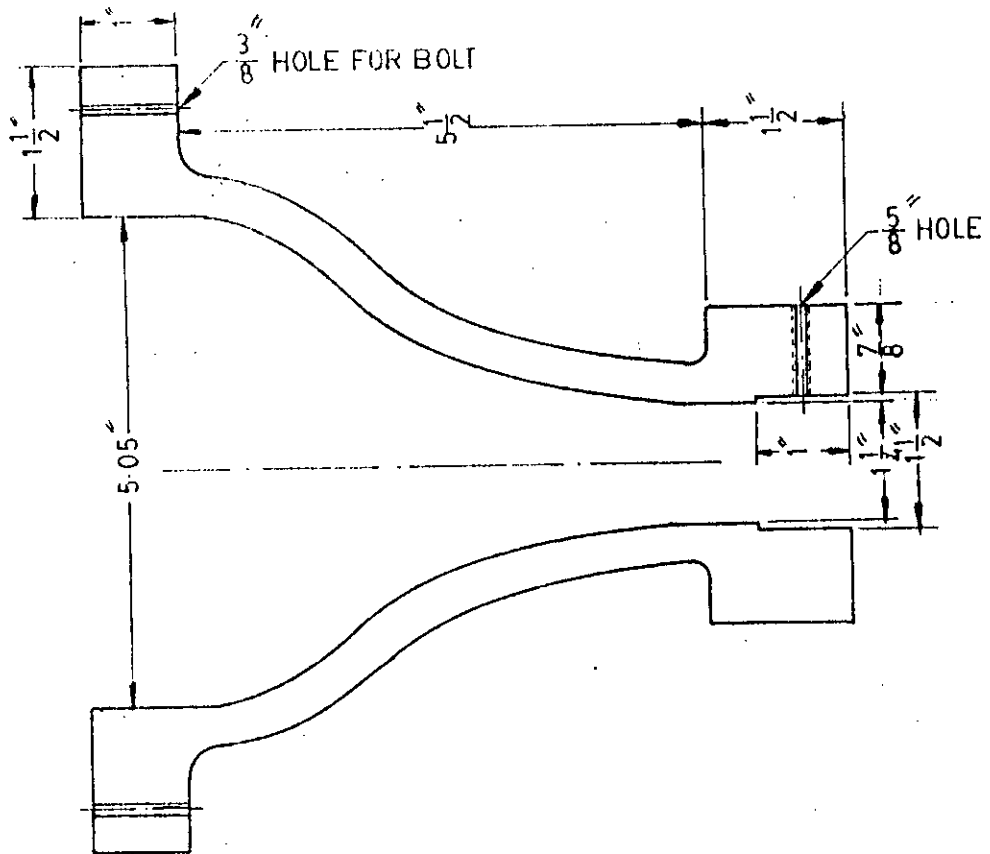


FIG. 4-5 a THE CONVERGING NOZZLE

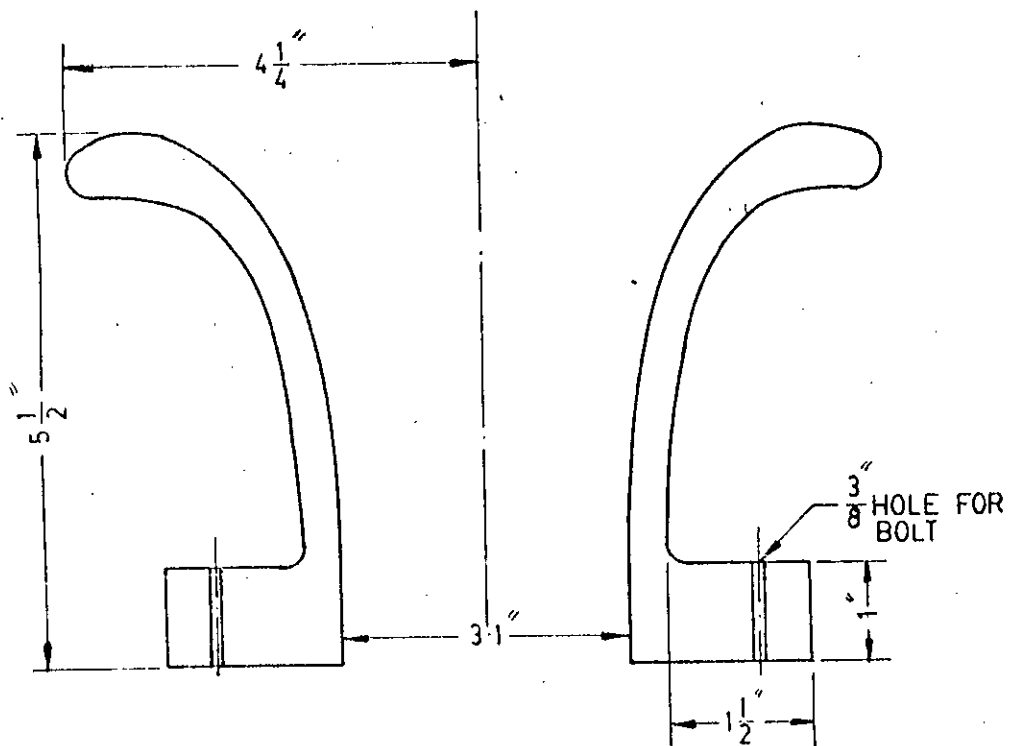


FIG. 4-5 b THE BELL MOUTH

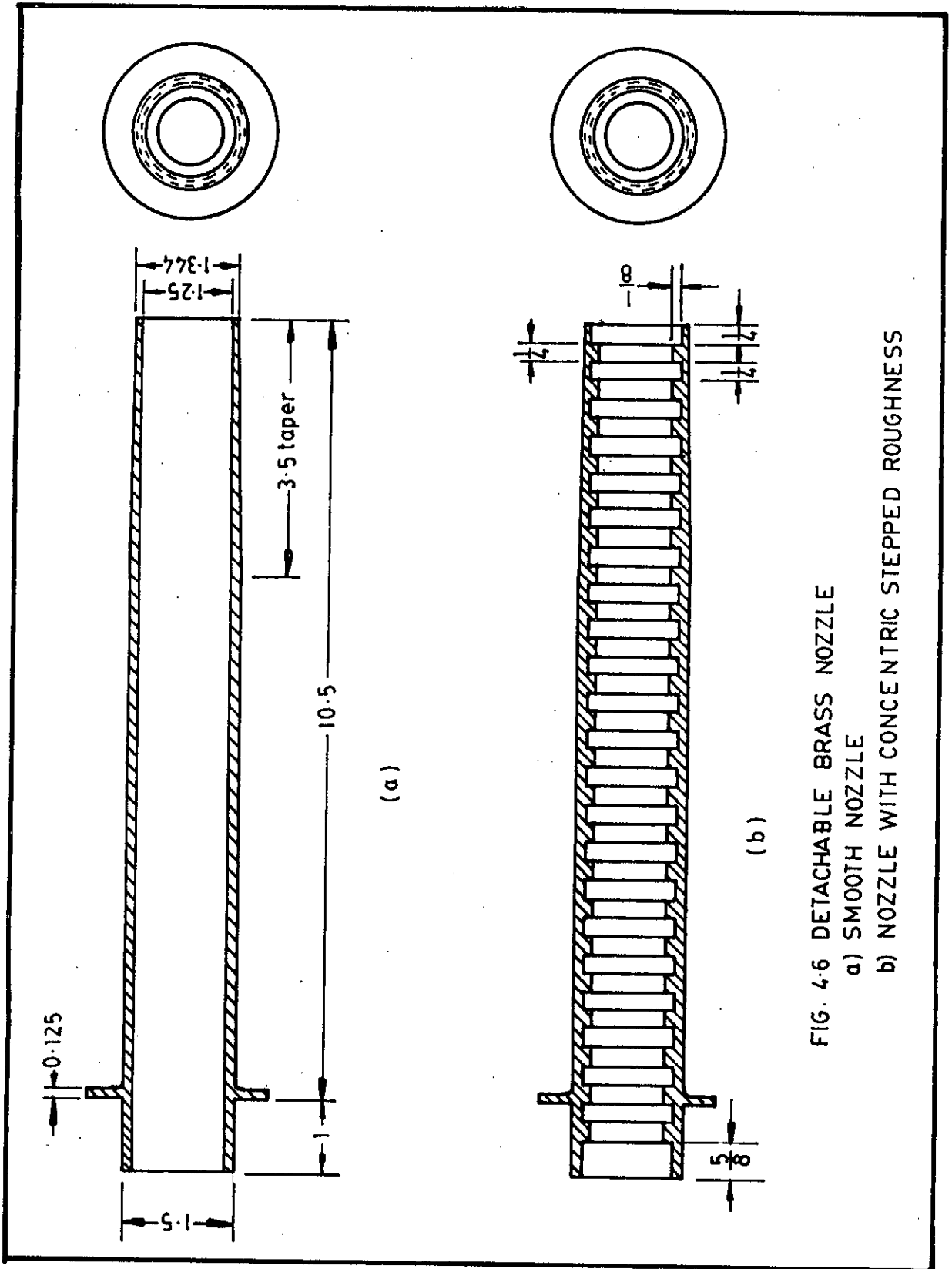


FIG. 4-6 DETACHABLE BRASS NOZZLE

a) SMOOTH NOZZLE

b) NOZZLE WITH CONCENTRIC STEPPED ROUGHNESS



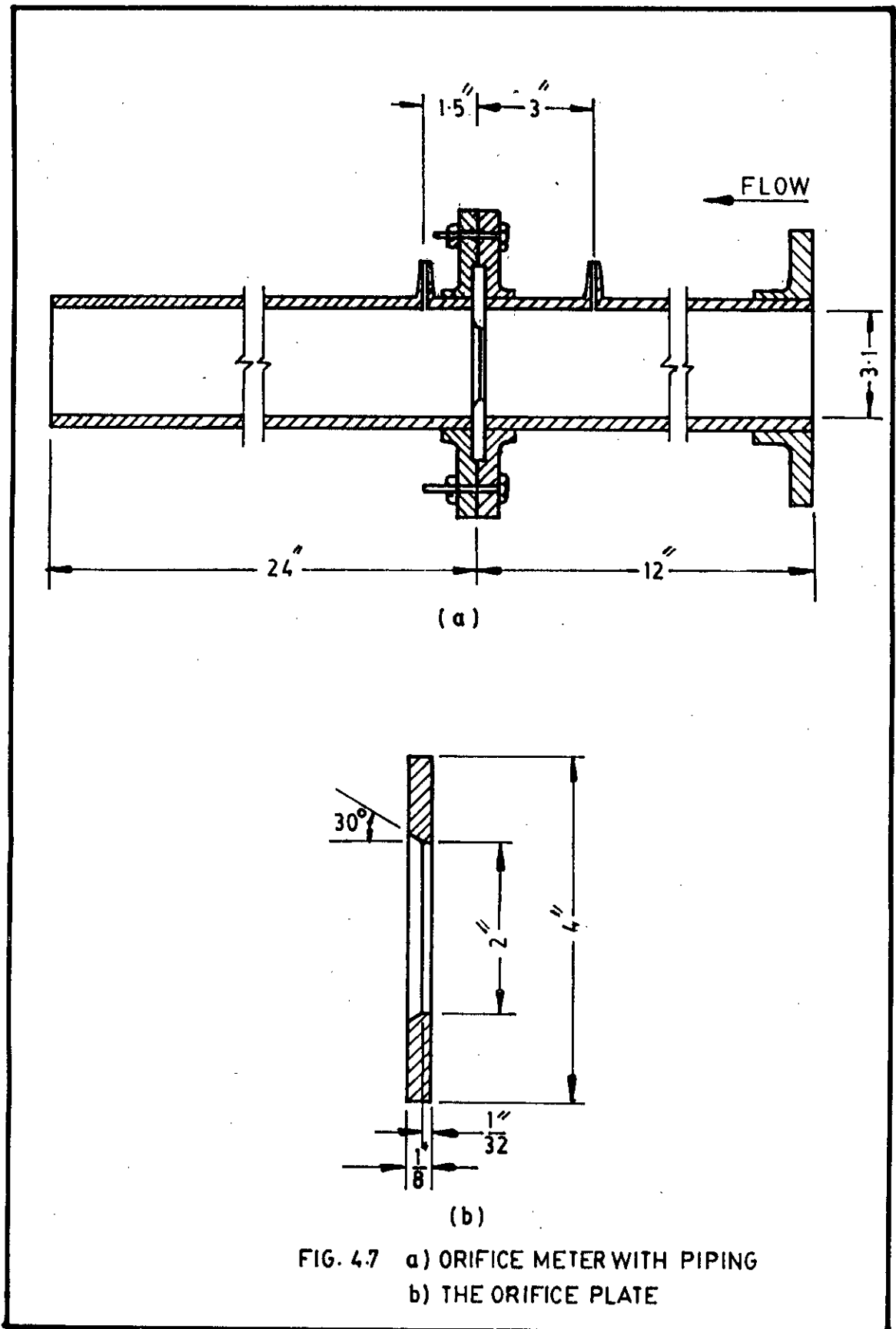


FIG. 4.7 a) ORIFICE METER WITH PIPING  
b) THE ORIFICE PLATE

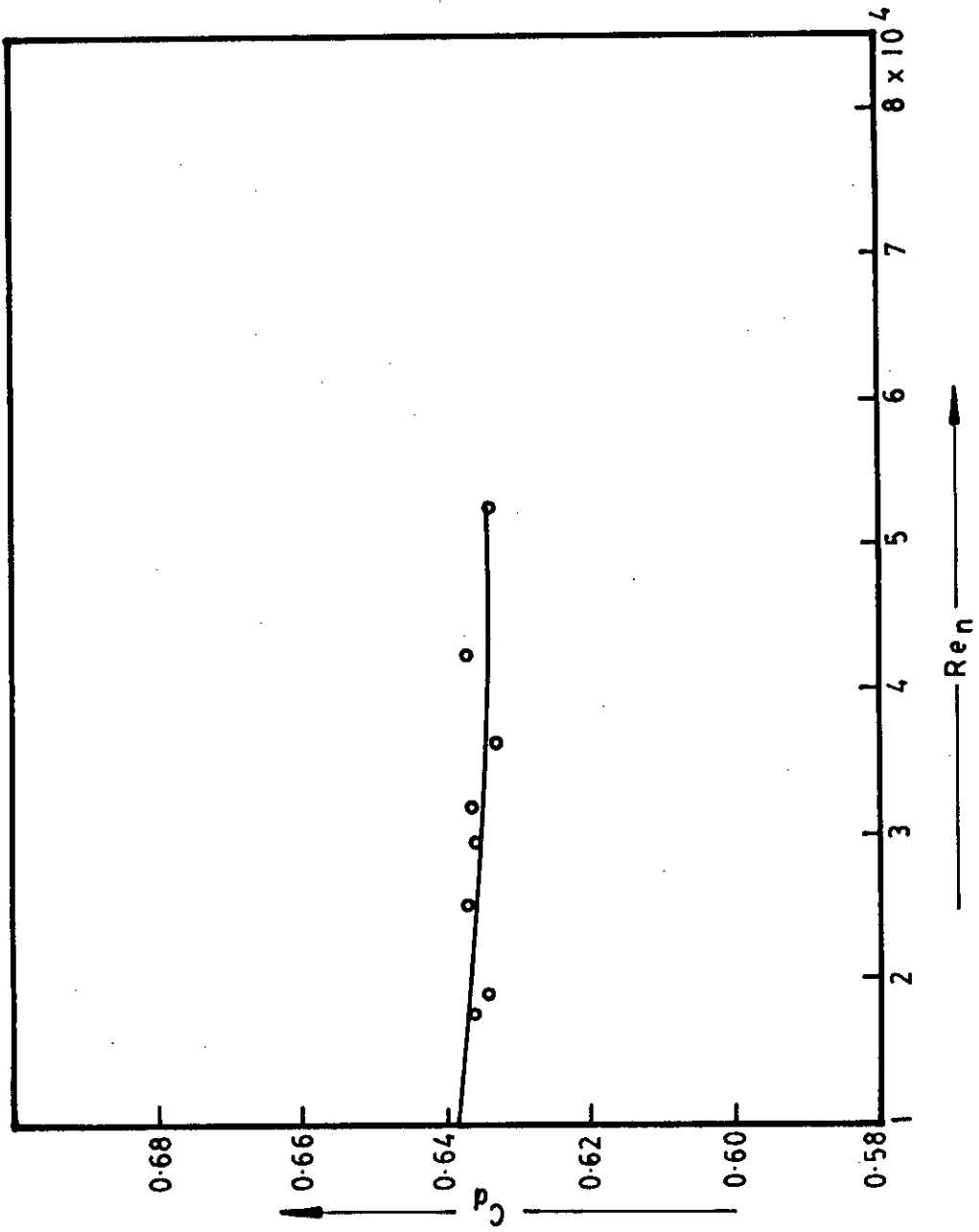


FIG. 4-8 CALIBRATION CURVE FOR ORIFICEMETER

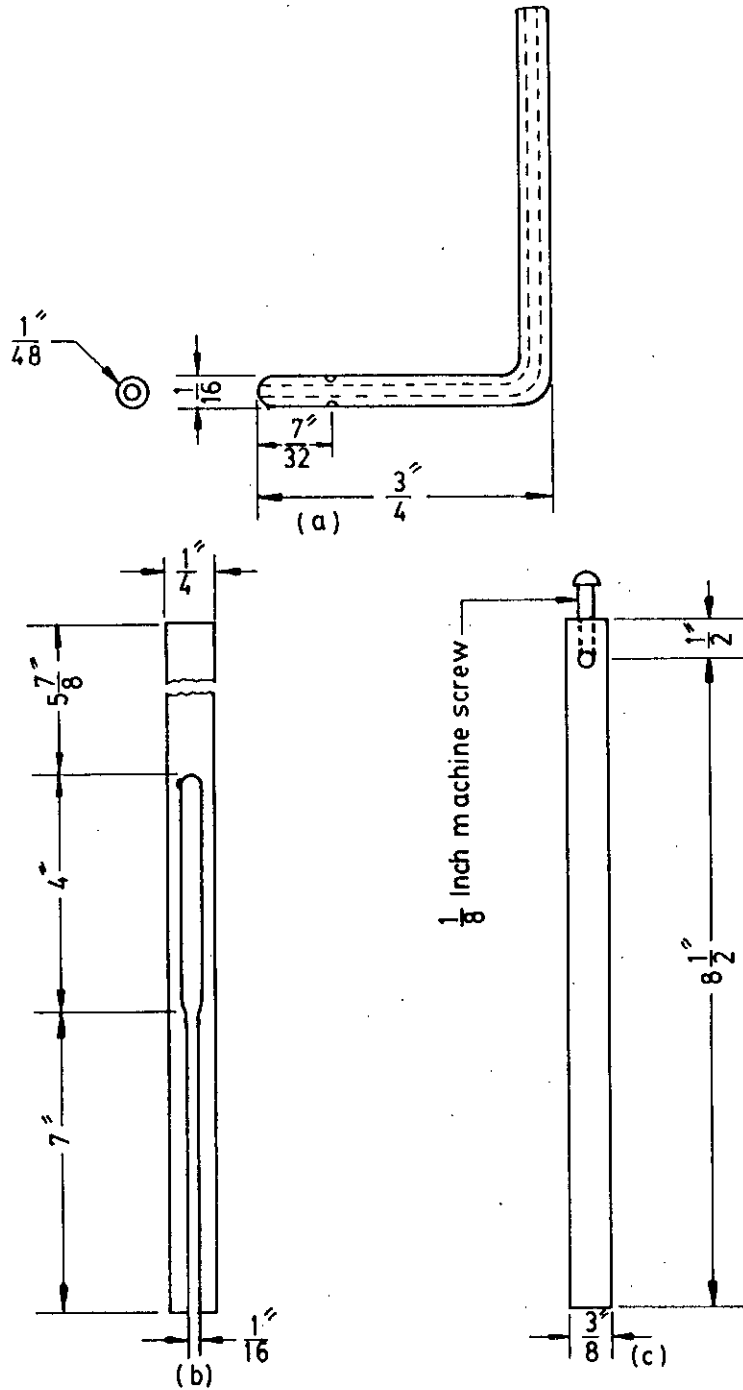


FIG. 4-9 PITOT TUBE & ATTACHMENTS

(a) PITOT STATIC TUBE (UNITED SENSOR)

(b) PITOT STATIC TUBE HOLDER

(c) HEIGHT GAGE ATTACHMENT

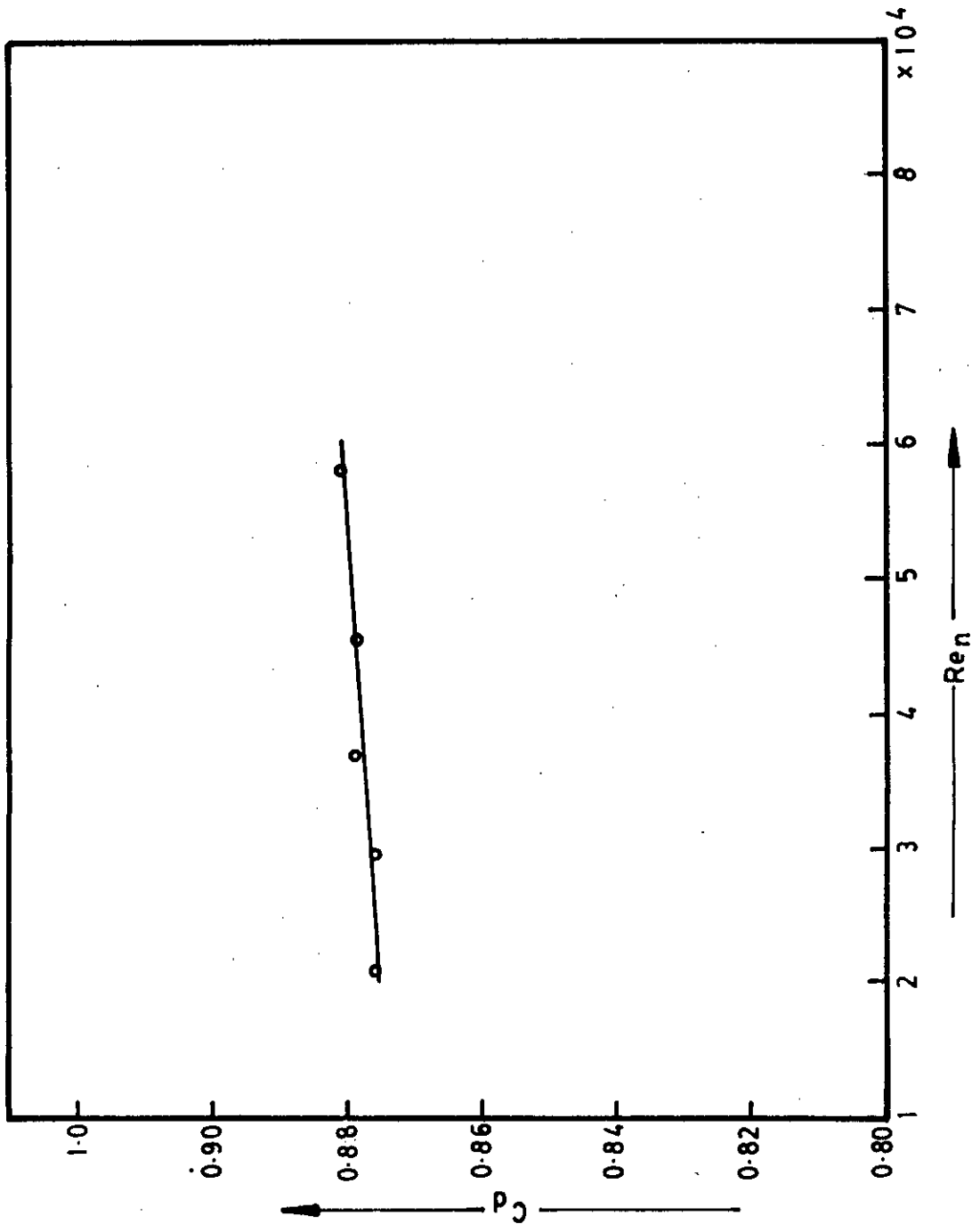


FIG. 4-10 CALIBRATION CURVE OF INLET NOZZLE

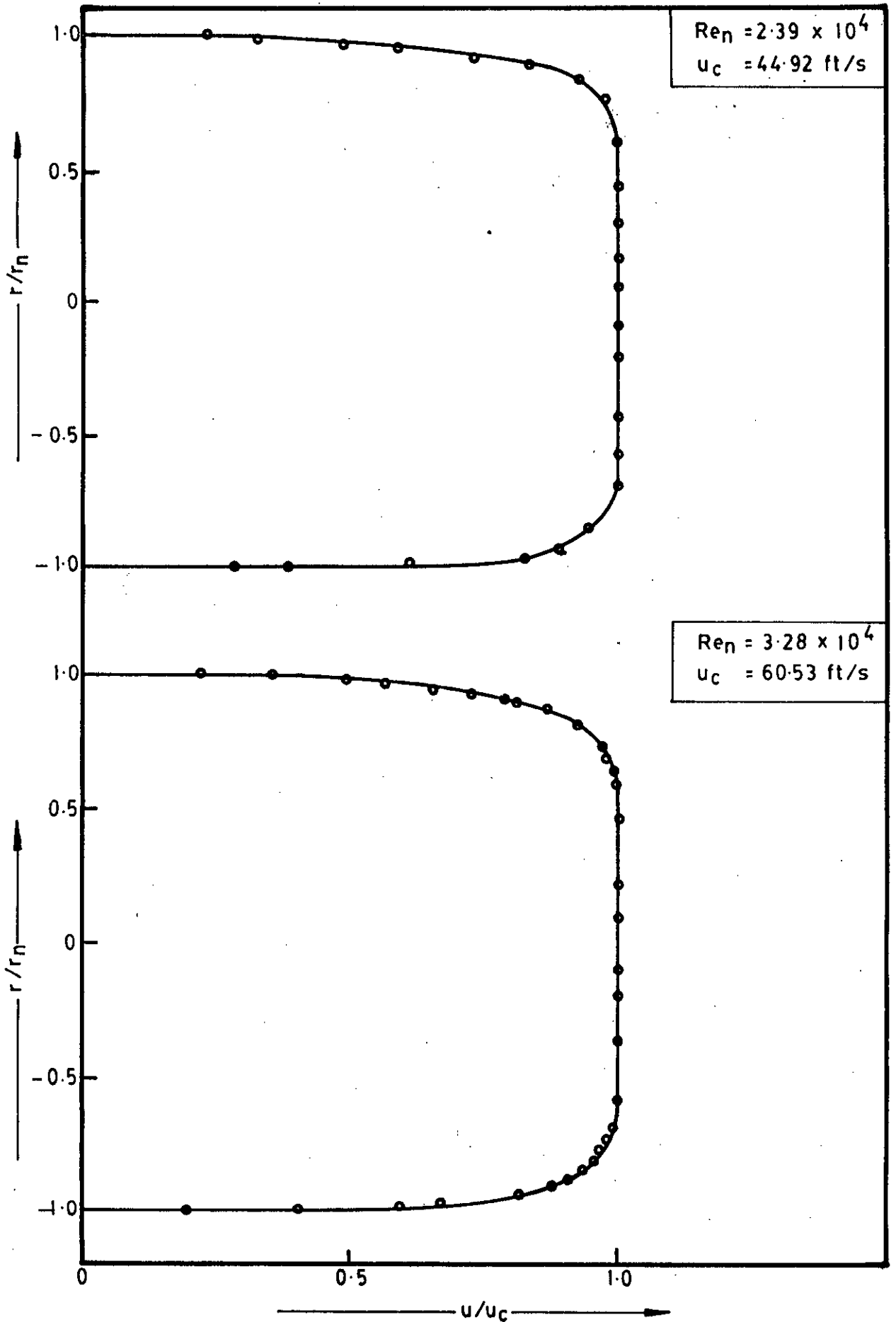


FIG. 5-1 EXIT VELOCITY PROFILE (SMOOTH NOZZLE)

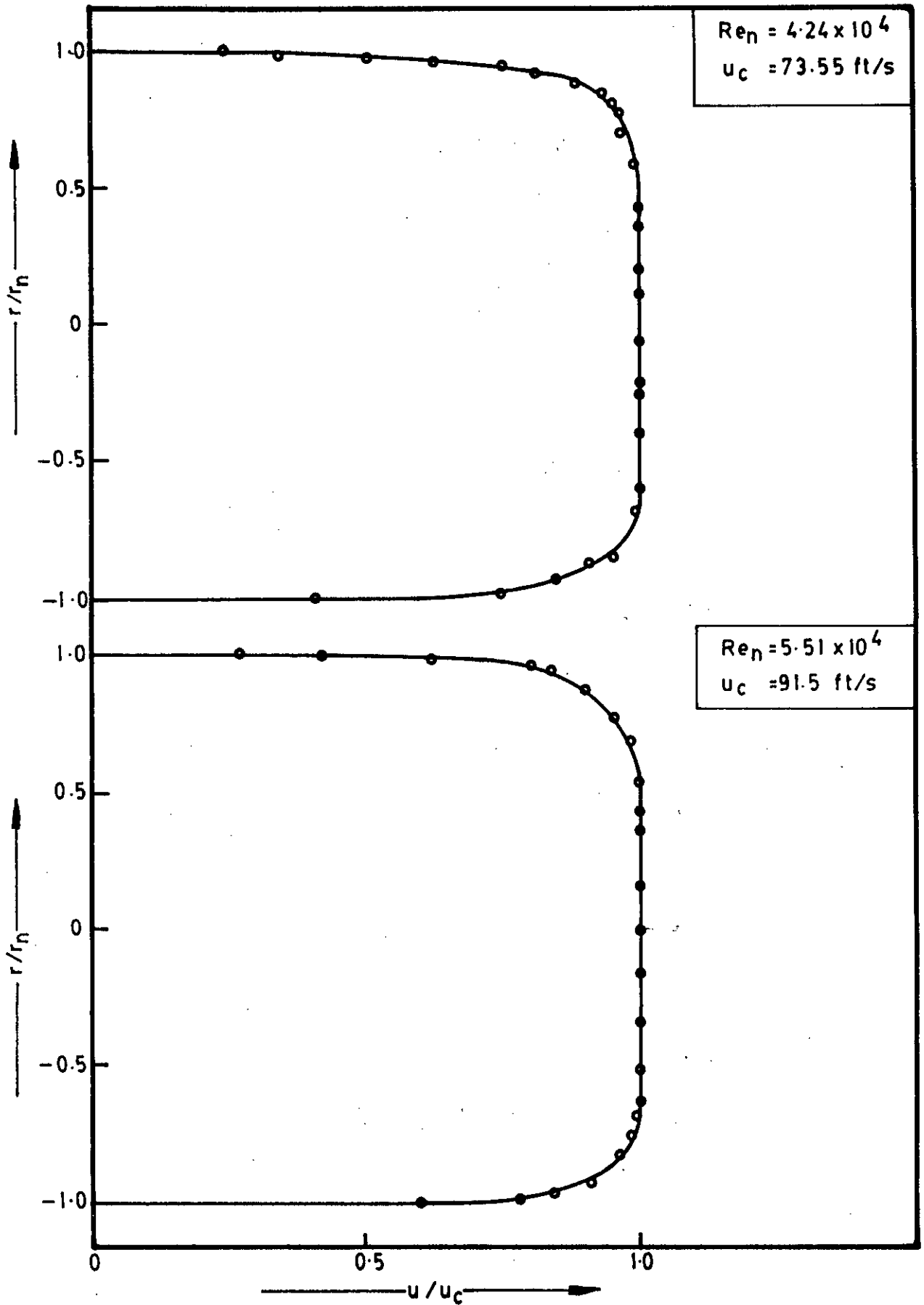


FIG. 5-1 (CONTINUED) EXIT VELOCITY PROFILE (SMOOTH NOZZLE)

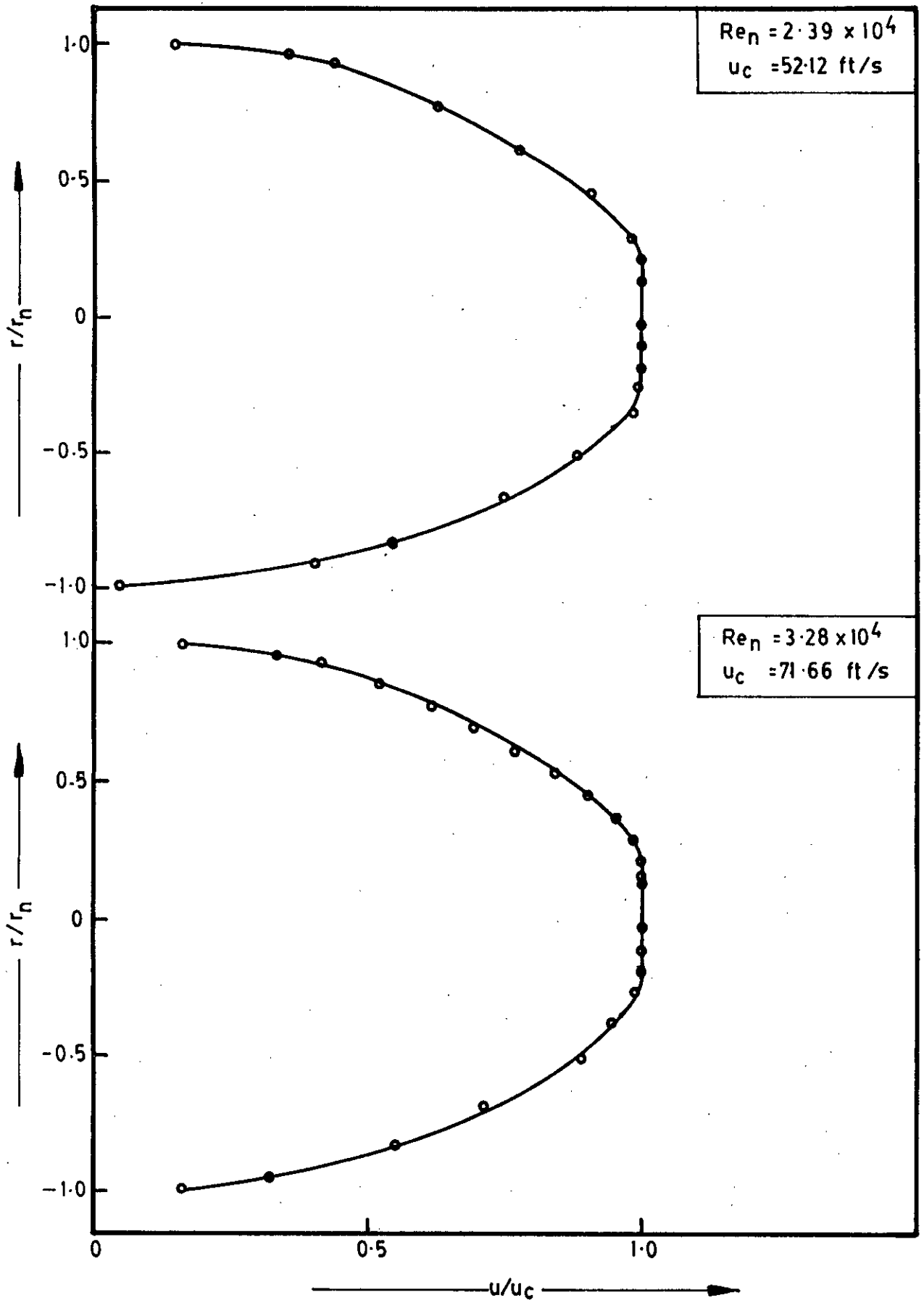
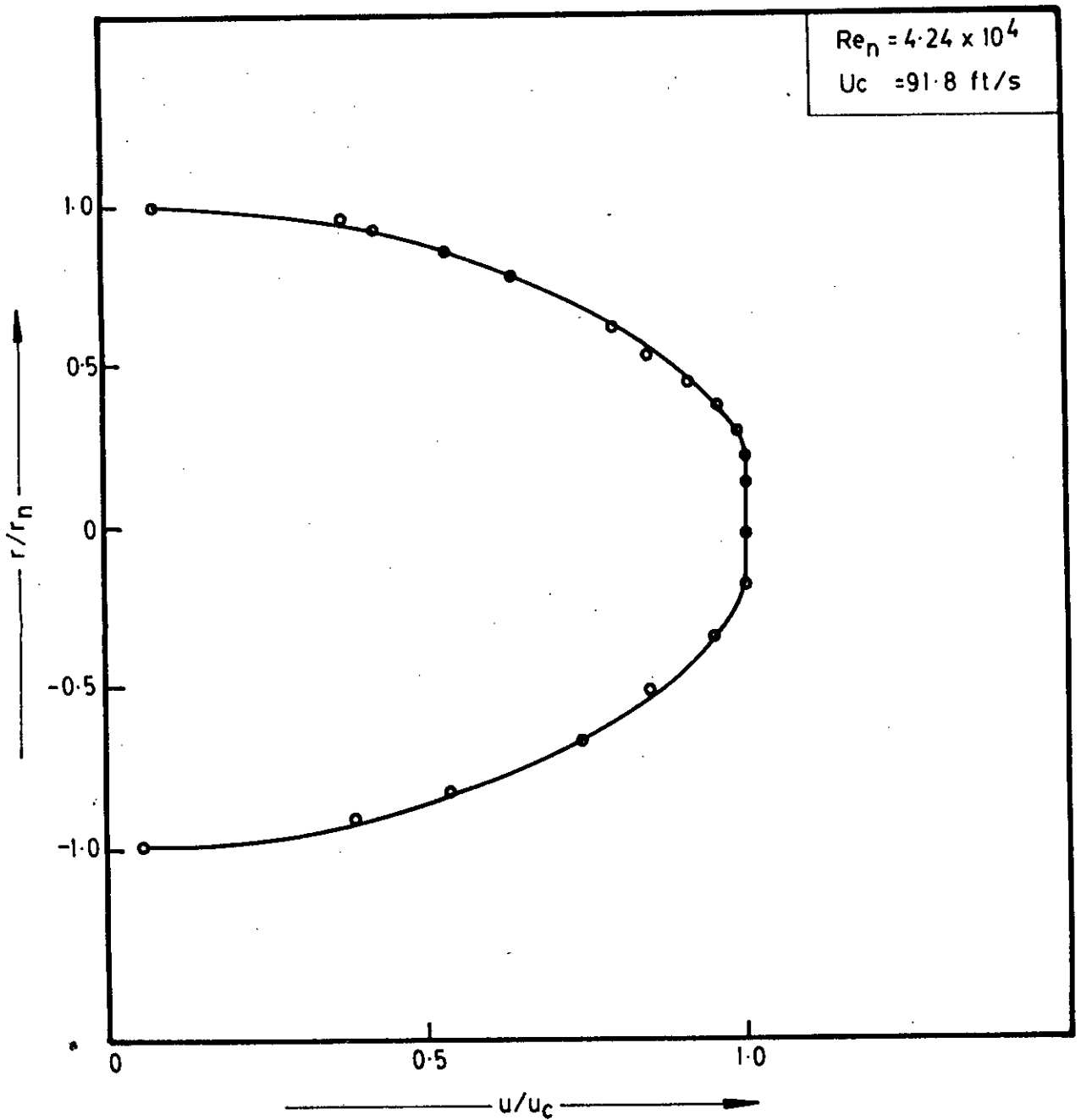


FIG. 5.2 EXIT VELOCITY PROFILE (NOZZLE ROUGHNESS  $\epsilon/D_n = 1/70$ )

FIG. 5.2 (CONTINUED) EXIT VELOCITY PROFILE (NOZZLE ROUGHNESS  $\epsilon/D_n = 1/70$ )



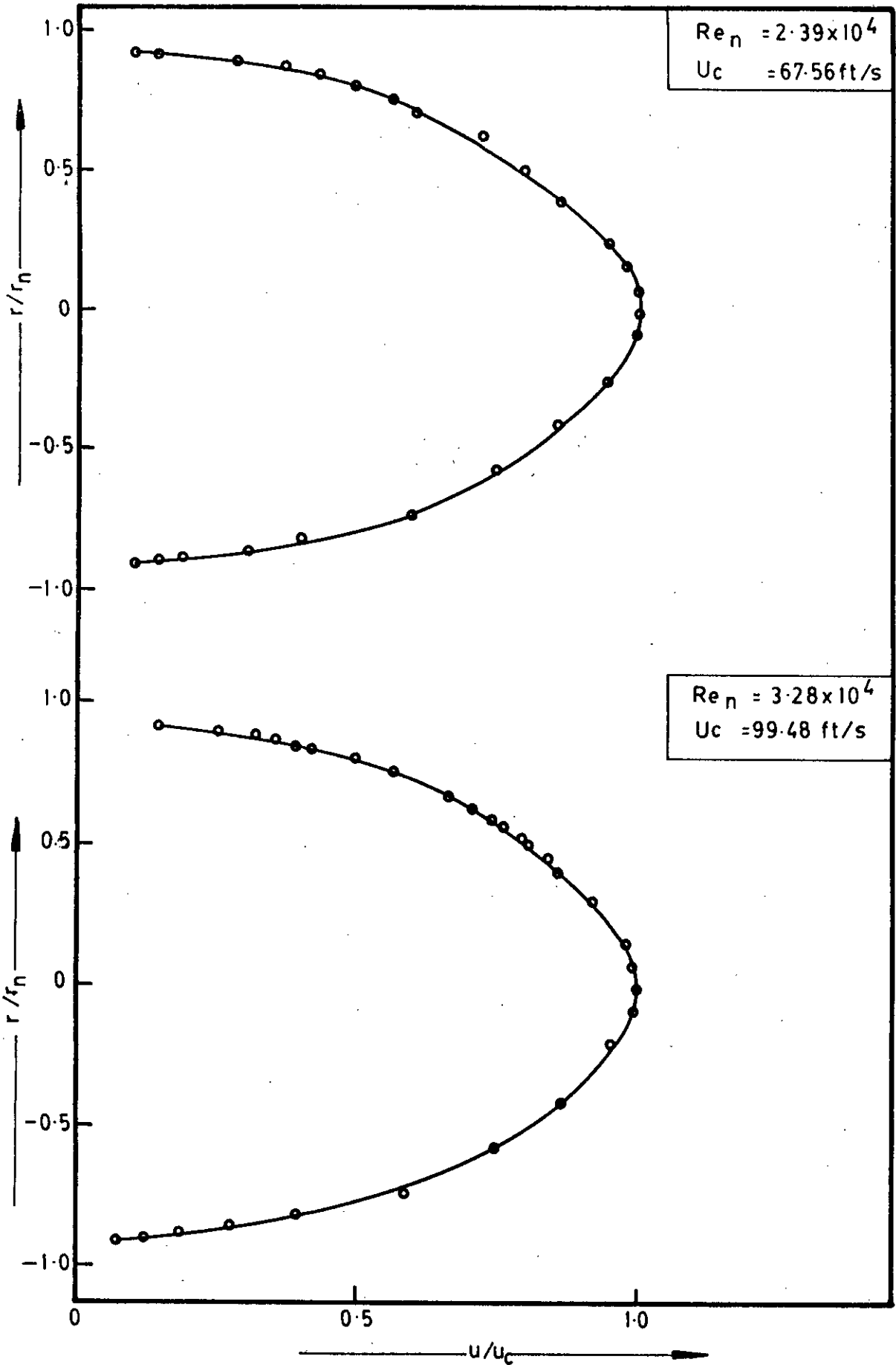


FIG. 5-3 EXIT VELOCITY PROFILES (NOZZLE ROUGHNESS  $\epsilon/D_n = 1/20$ )

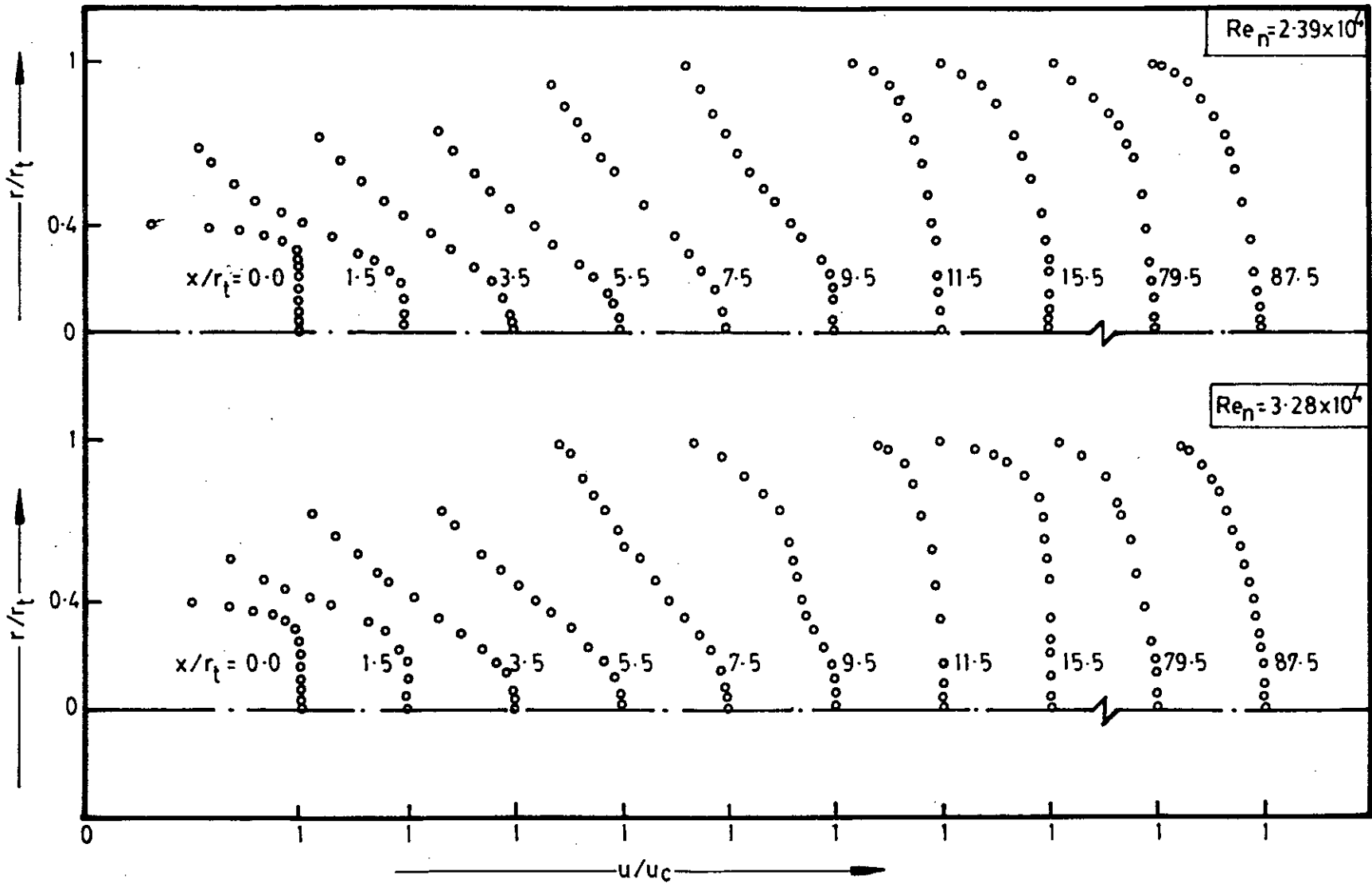


FIG. 5.4 MEAN VELOCITY PROFILE (SMOOTH NOZZLE)

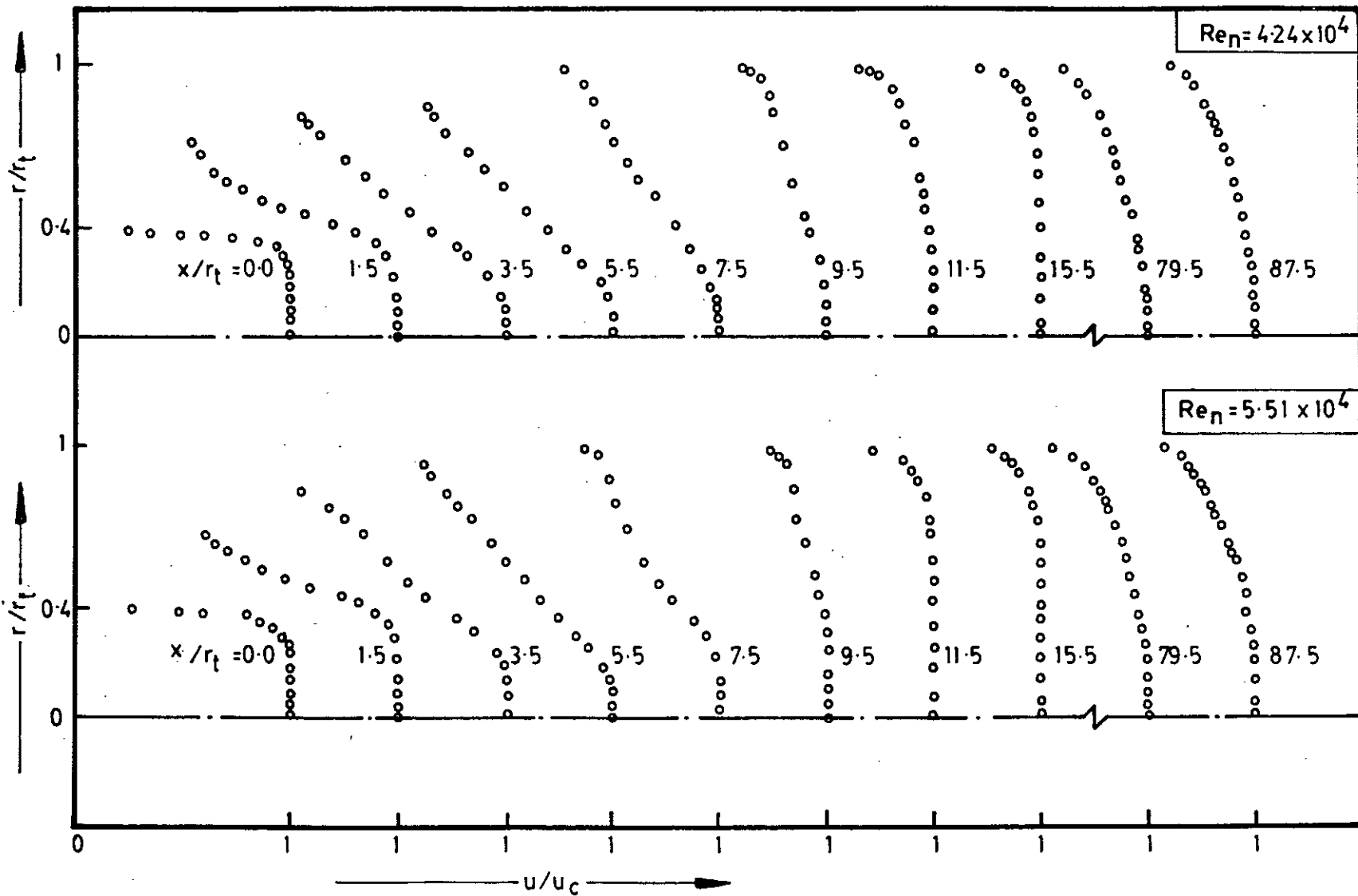


FIG. 5-4 (CONTINUED) MEAN VELOCITY PROFILE (SMOOTH NOZZLE)

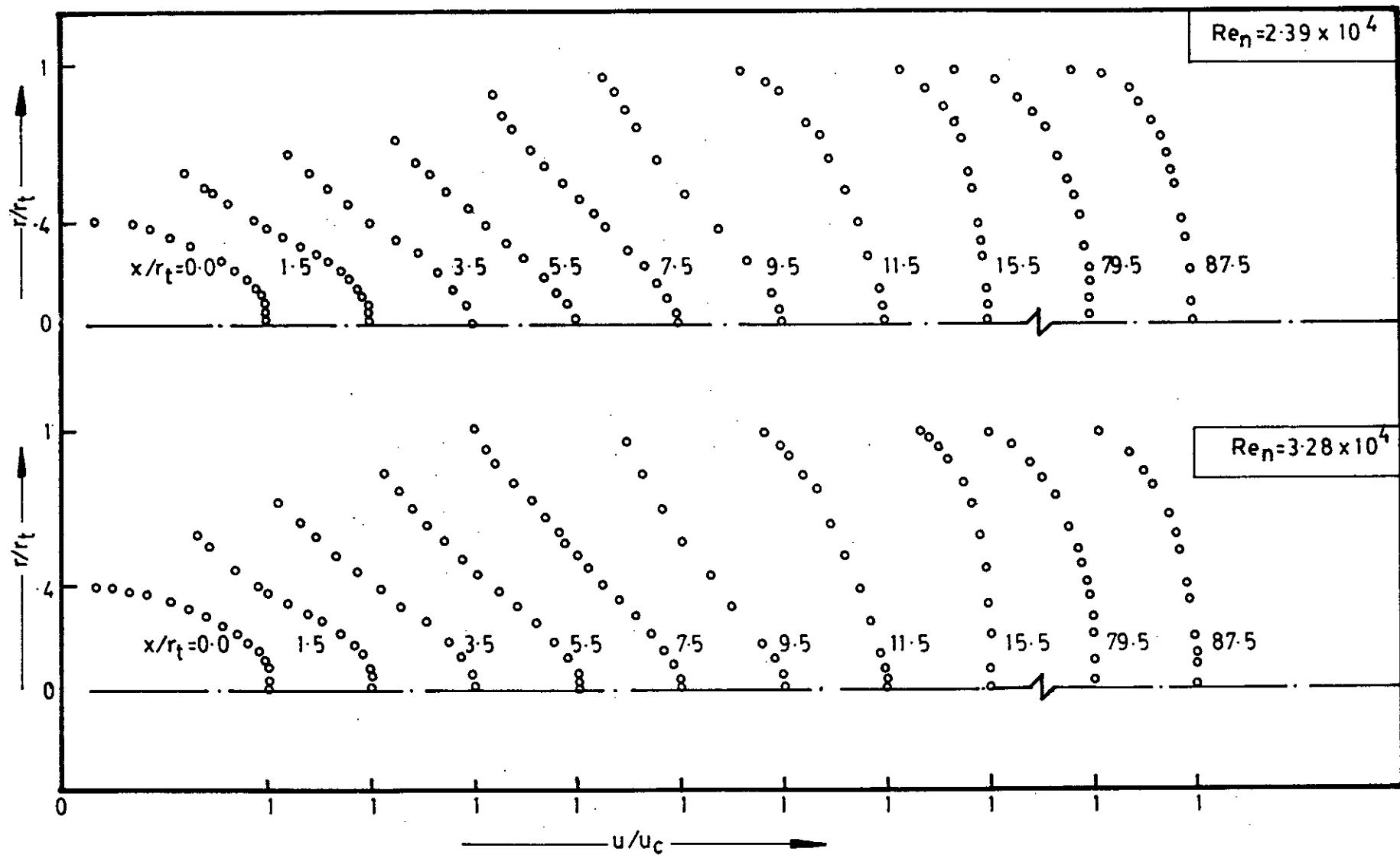


FIG. 5.5 MEAN VELOCITY PROFILE (NOZZLE ROUGHNESS = 1/70)

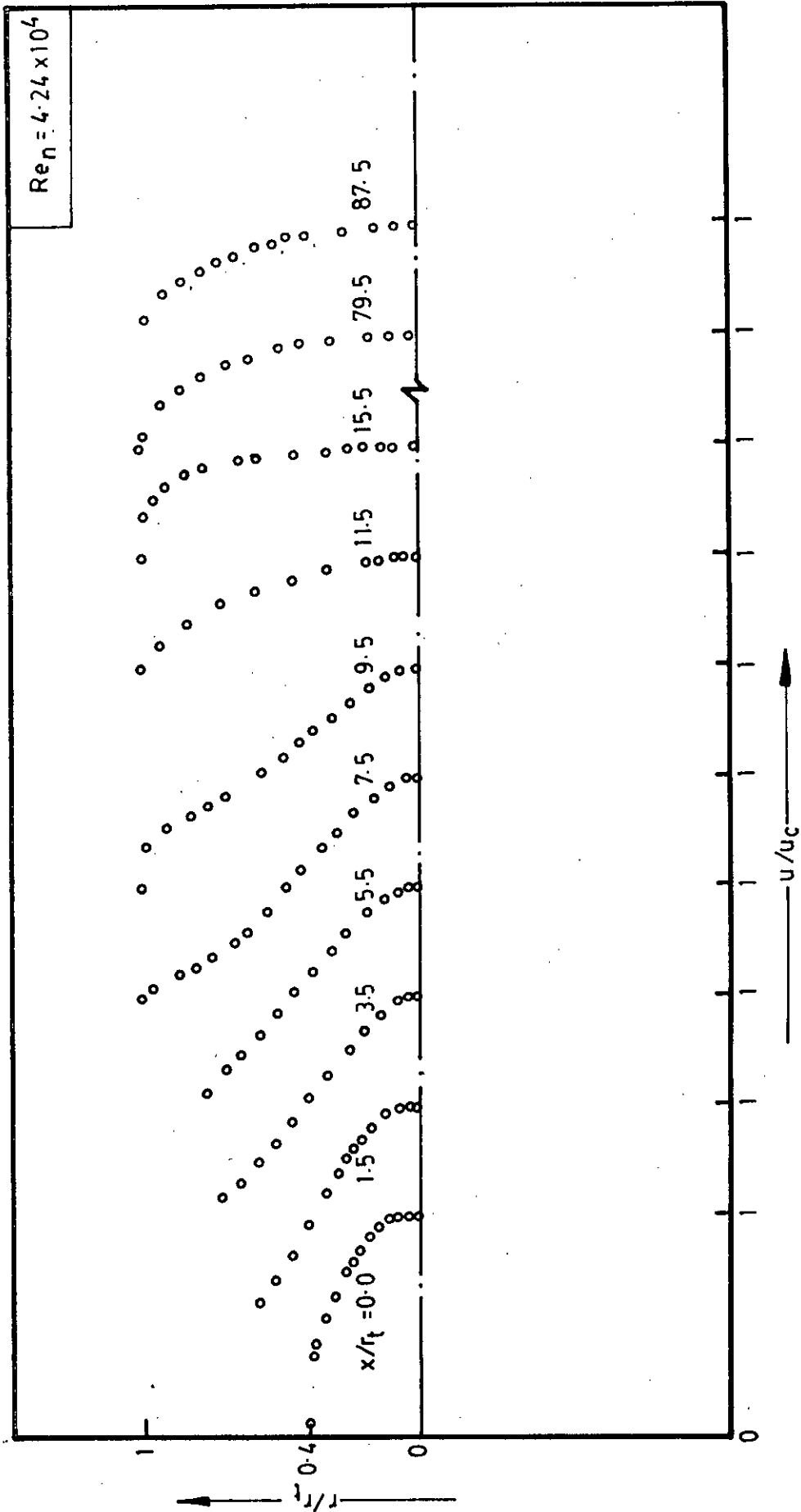


FIG. 5.5 (CONTINUED) MEAN VELOCITY PROFILES (NOZZLE ROUGHNESS = 1/70)

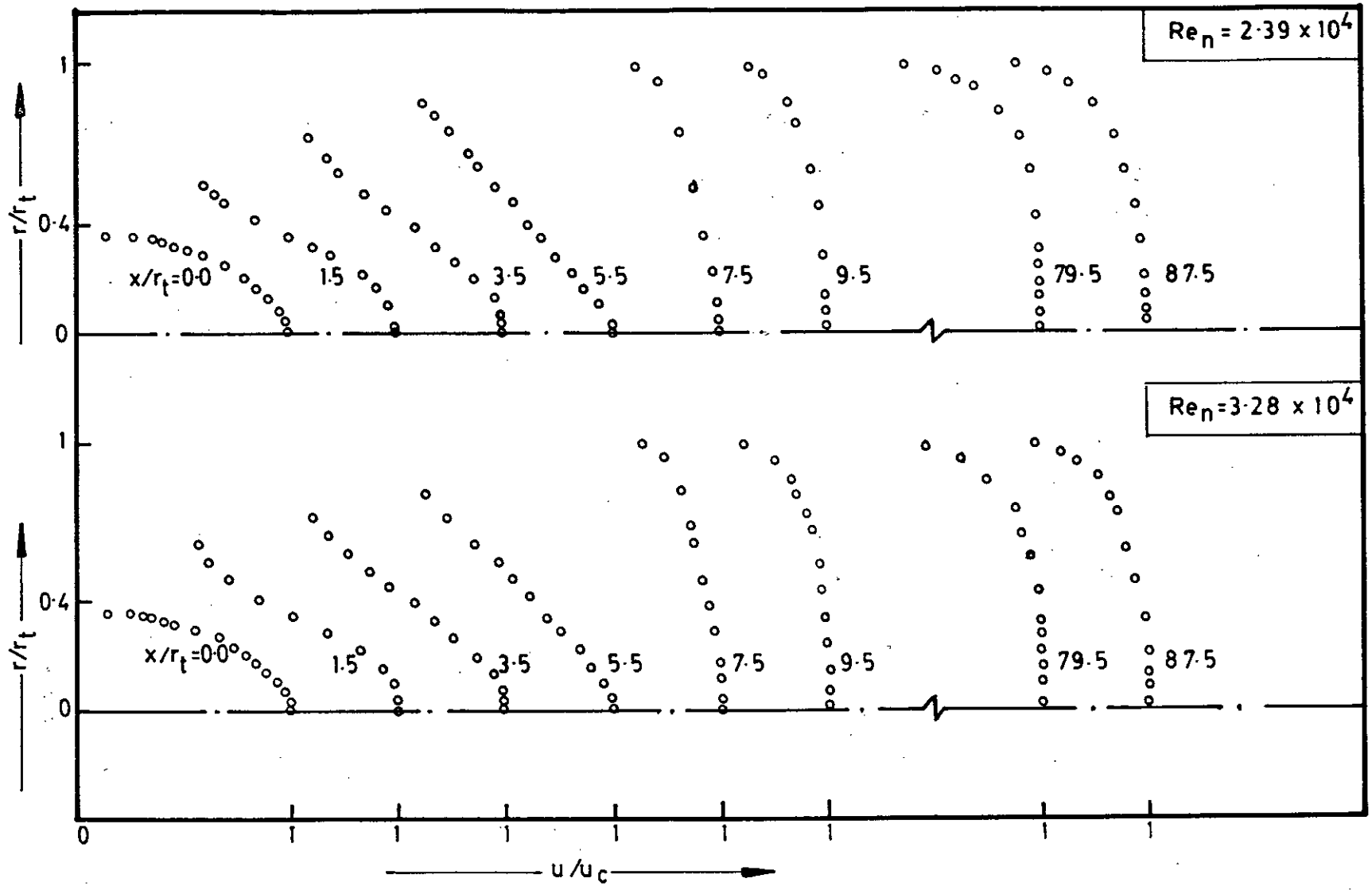


FIG. 5.6 MEAN VELOCITY PROFILES (NOZZLE ROUGHNESS = 1/20)

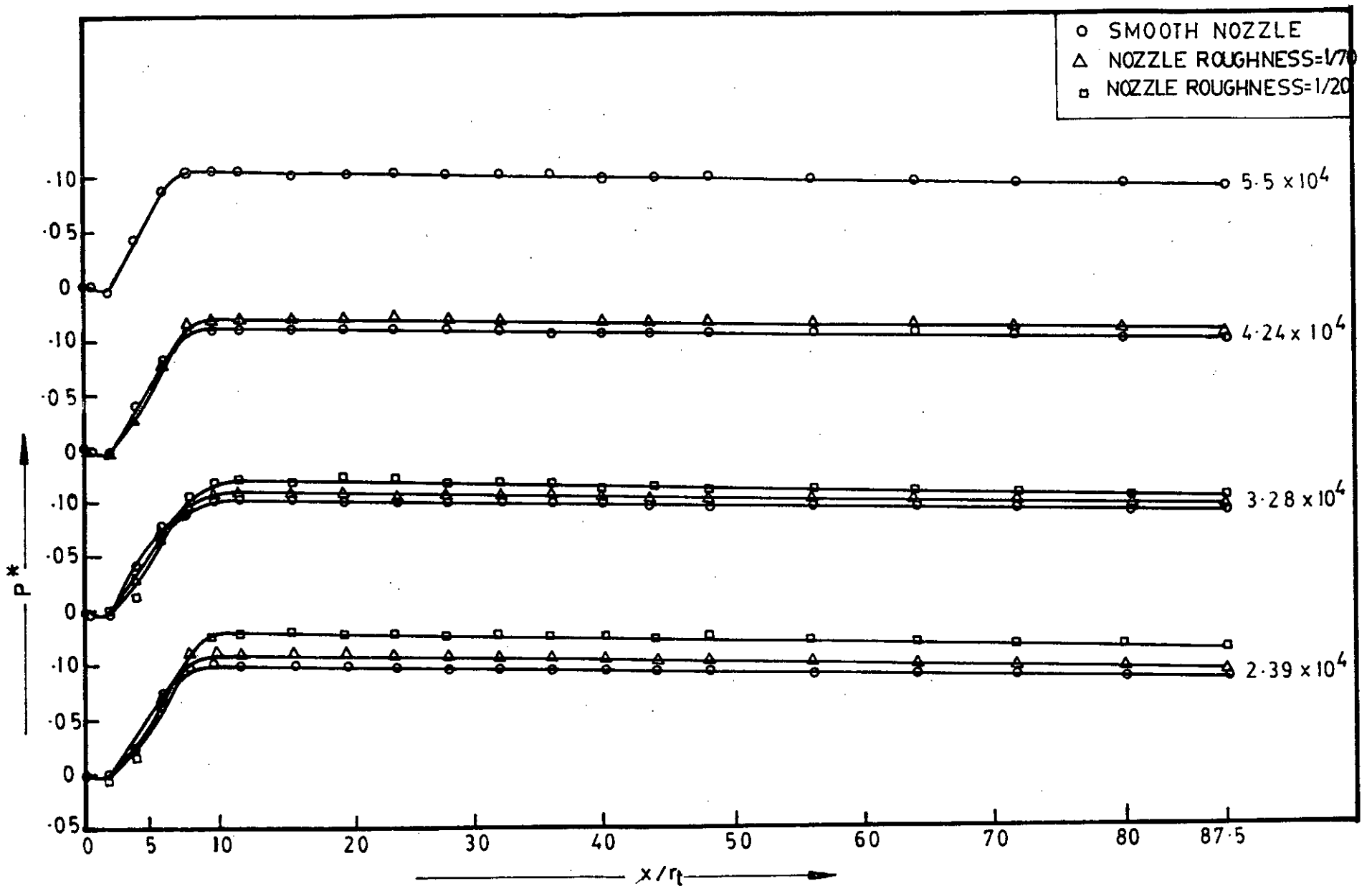


FIG. 57 STATIC PRESSURE DISTRIBUTION WITH AXIAL DISTANCE

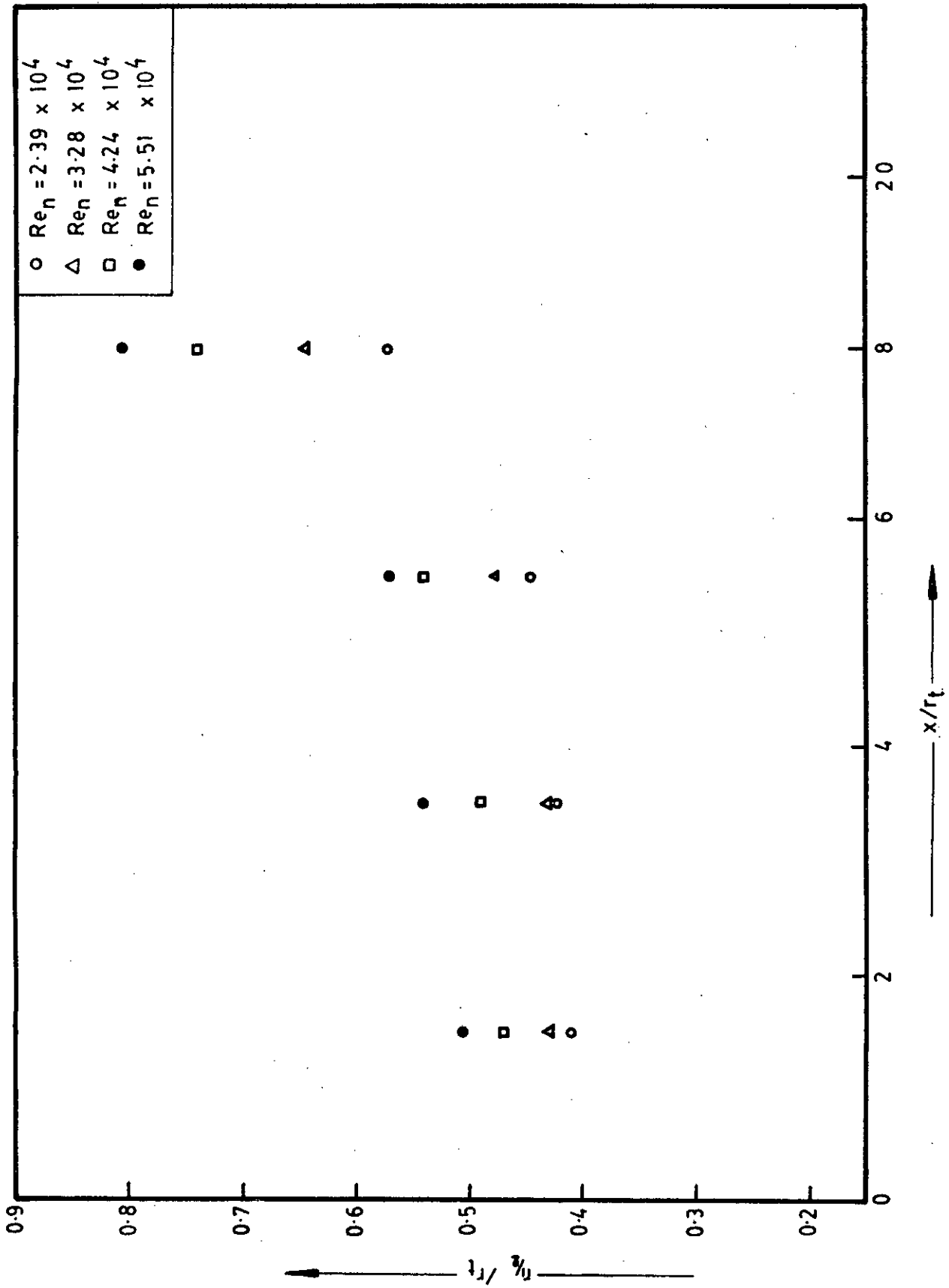


FIG. 5-8 VARIATION OF HALF-RADIUS WITH AXIAL DISTANCE (SMOOTH NOZZLE)



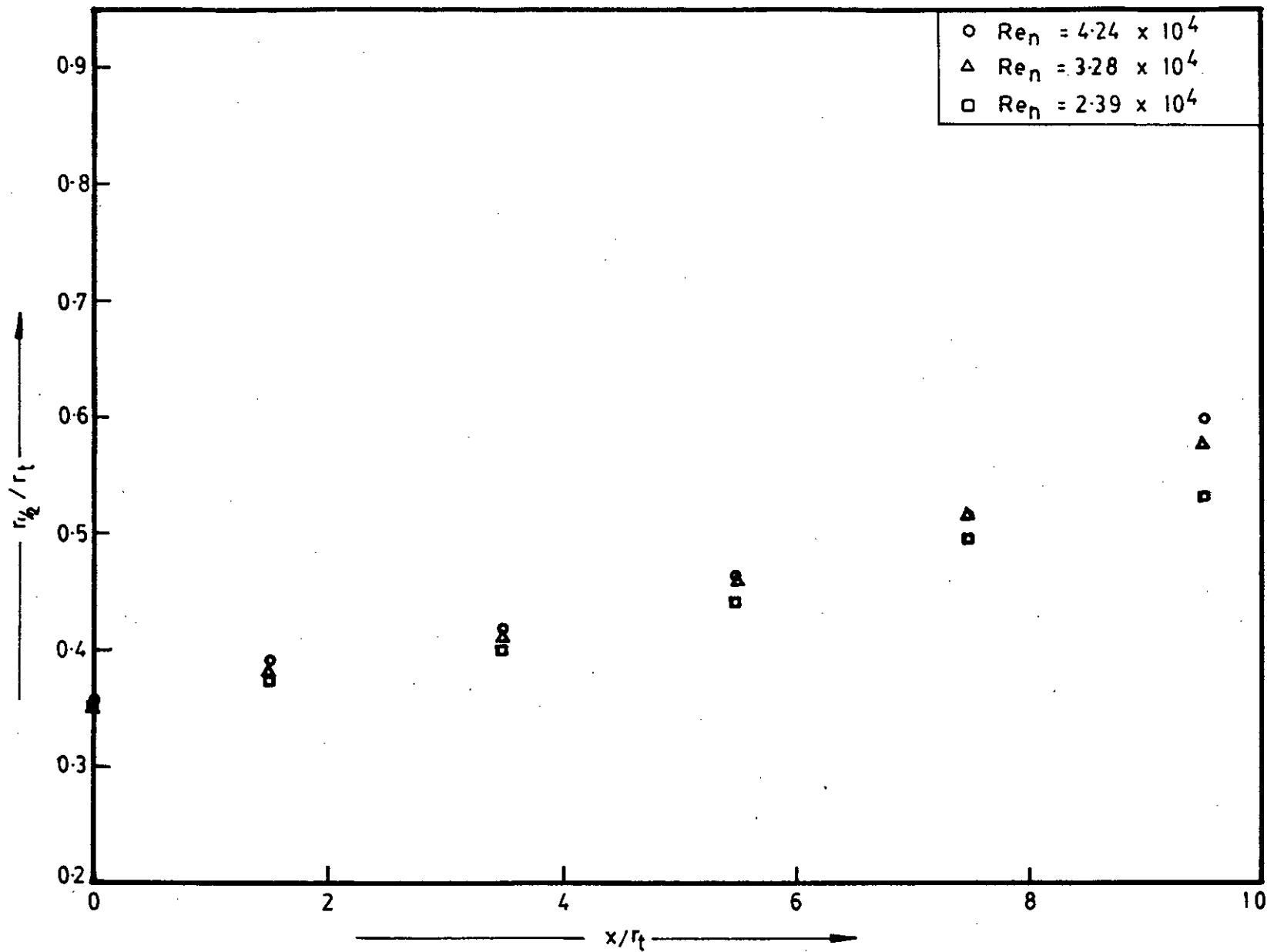


FIG. 5-9 VARIATION OF HALF-RADIUS WITH AXIAL DISTANCE (NOZZLE ROUGHNESS = 1/70)

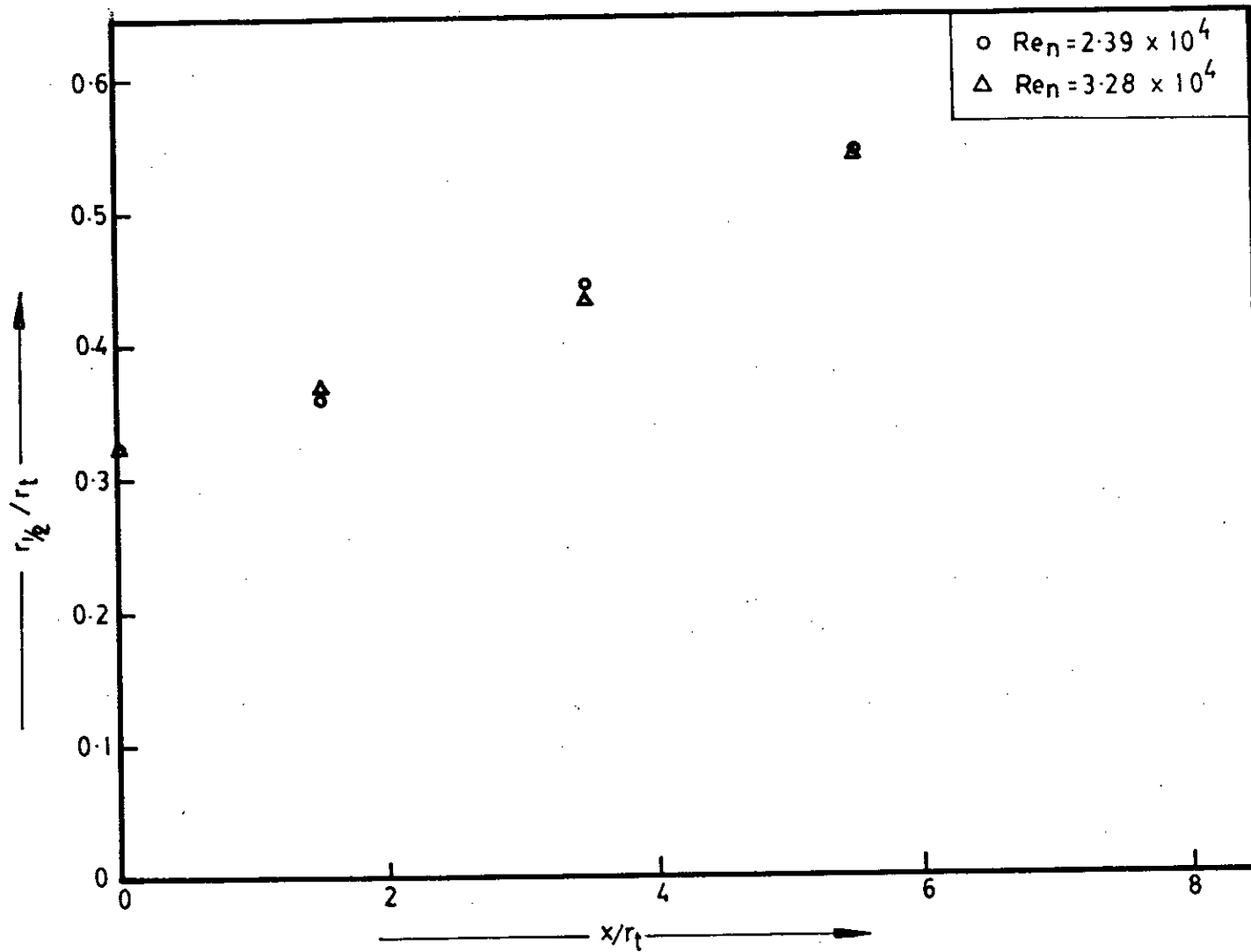


FIG. 5-10 VARIATION OF HALF-RADIUS WITH AXIAL DISTANCE (NOZZLE ROUGHNESS  $\epsilon/D_n = 1/20$ )

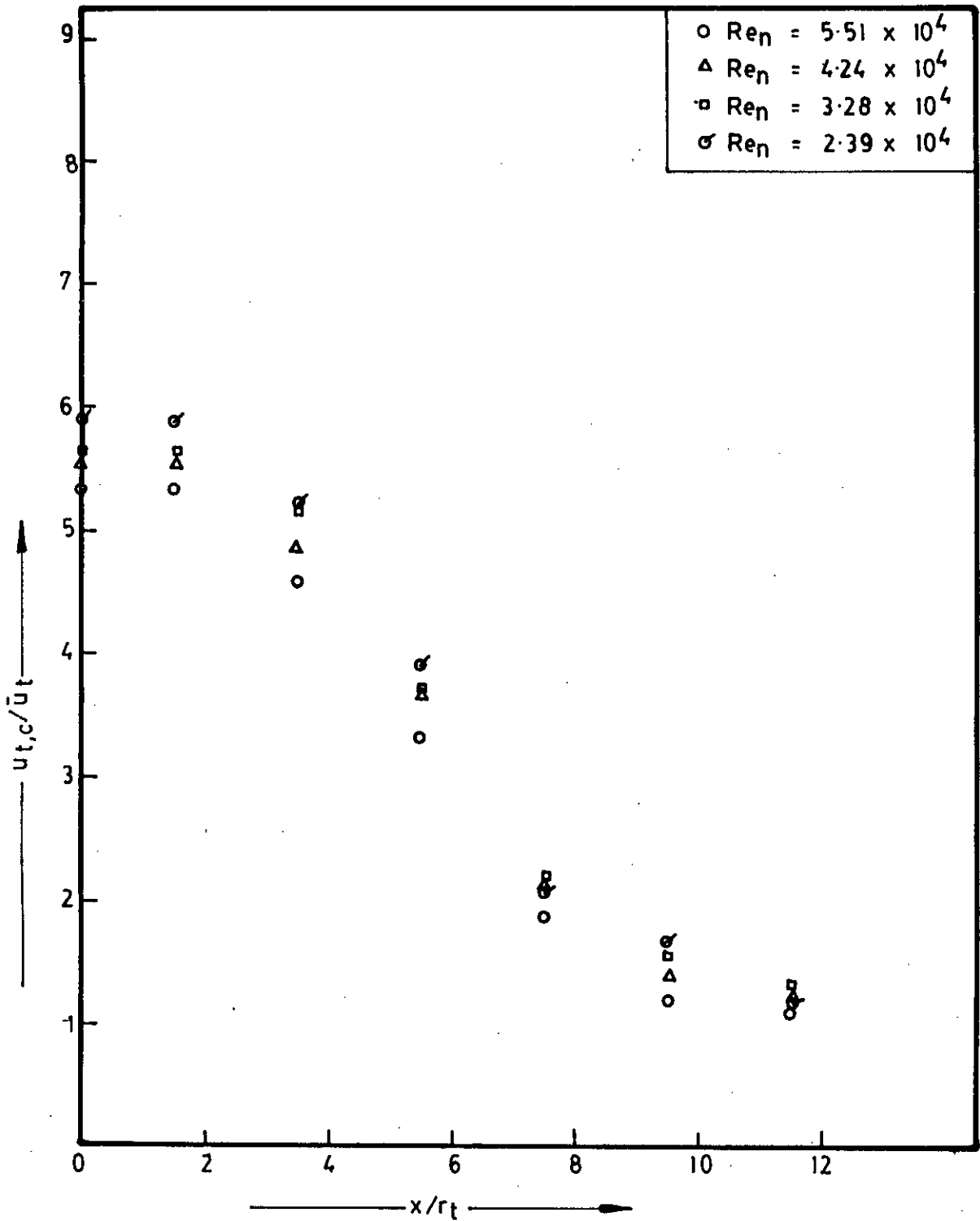


FIG. 5.11 DISTRIBUTION OF CENTRE LINE VELOCITY (SMOOTH NOZZLE)

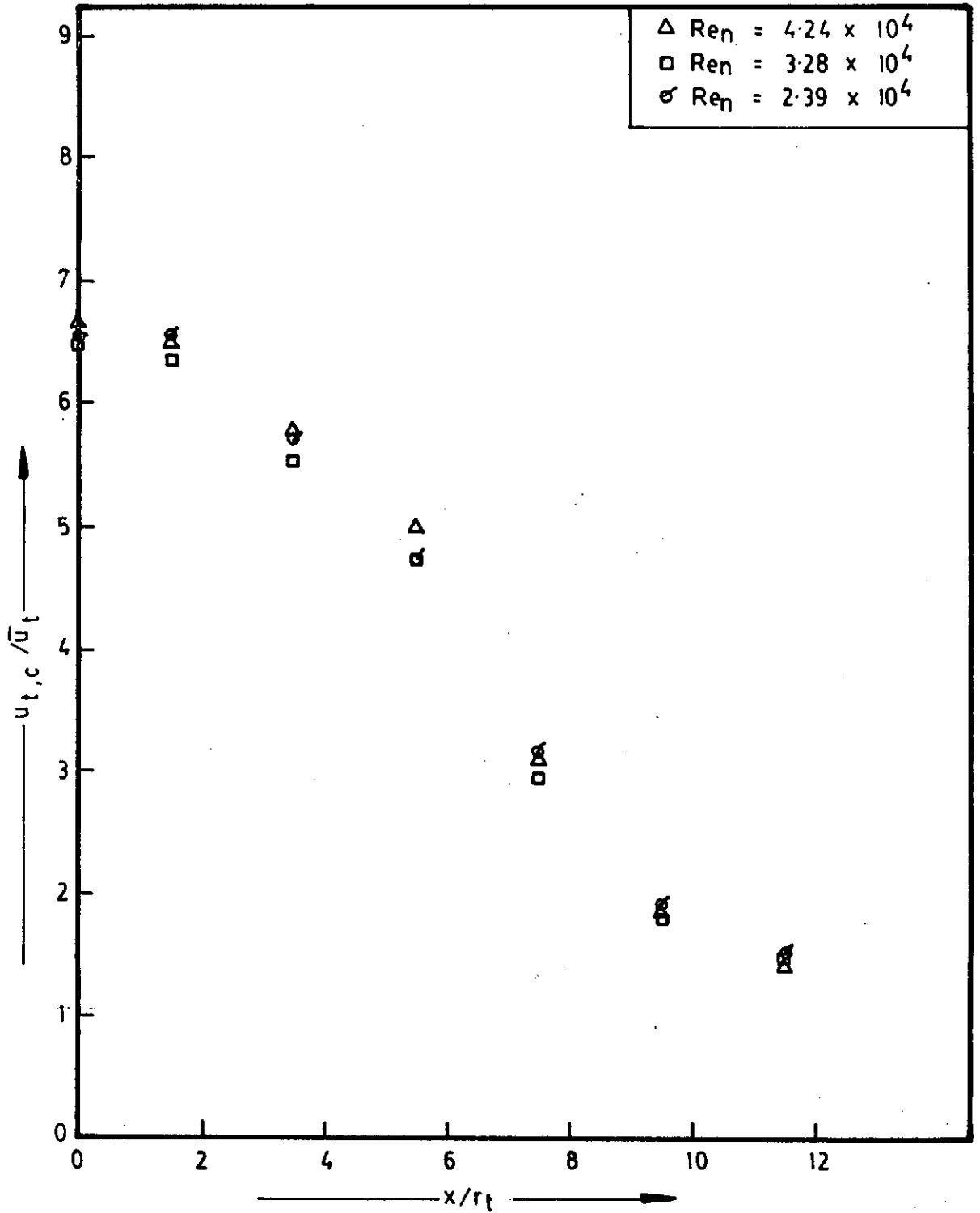


FIG. 5-12 DISTRIBUTION OF CENTRE LINE VELOCITY (NOZZLE ROUGHNESS  $\epsilon / D_n = 1/70$ )

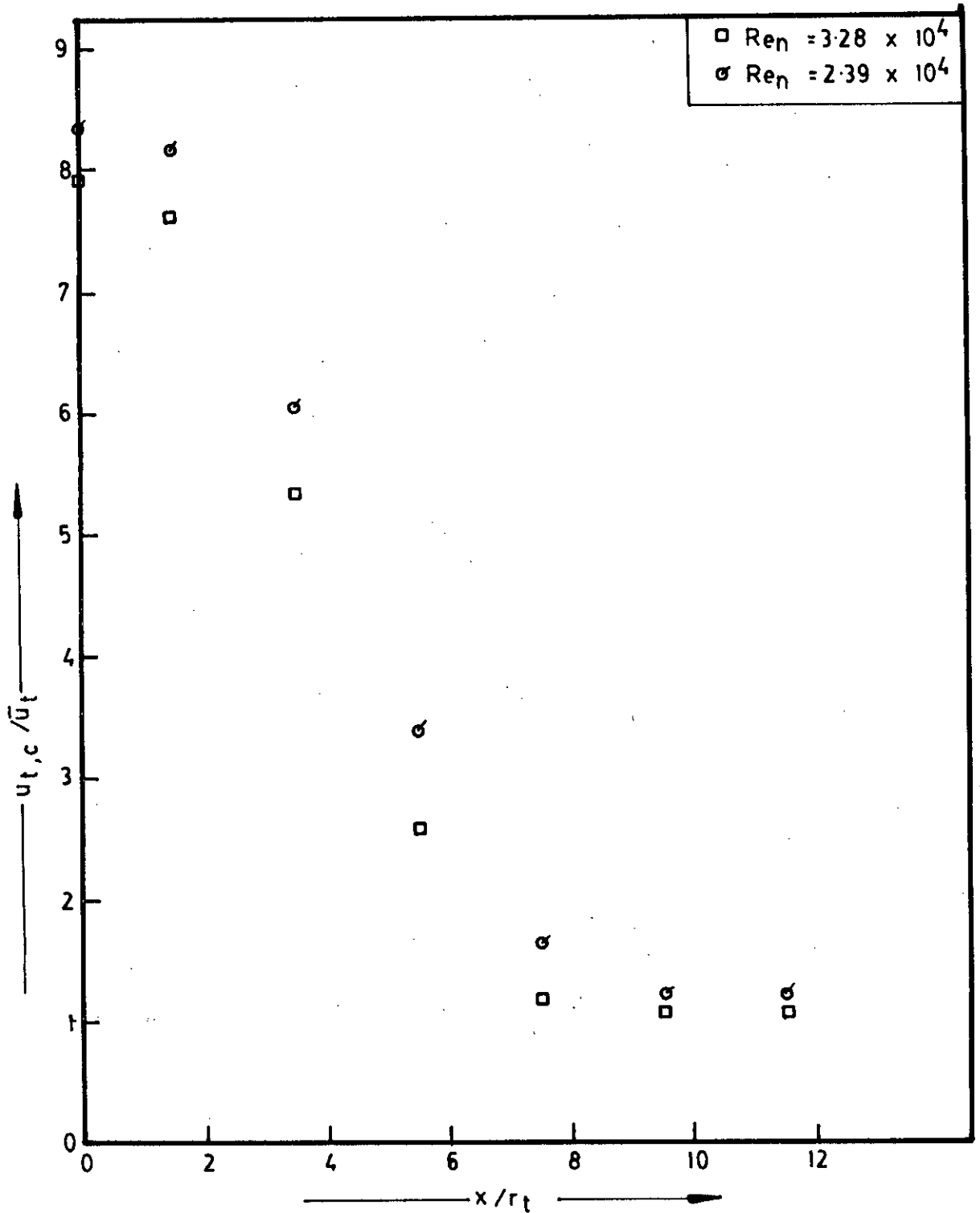


FIG. 5-13 DISTRIBUTION OF CENTRE LINE VELOCITY (NOZZLE ROUGHNESS  $\epsilon/D_n = 1/20$ )

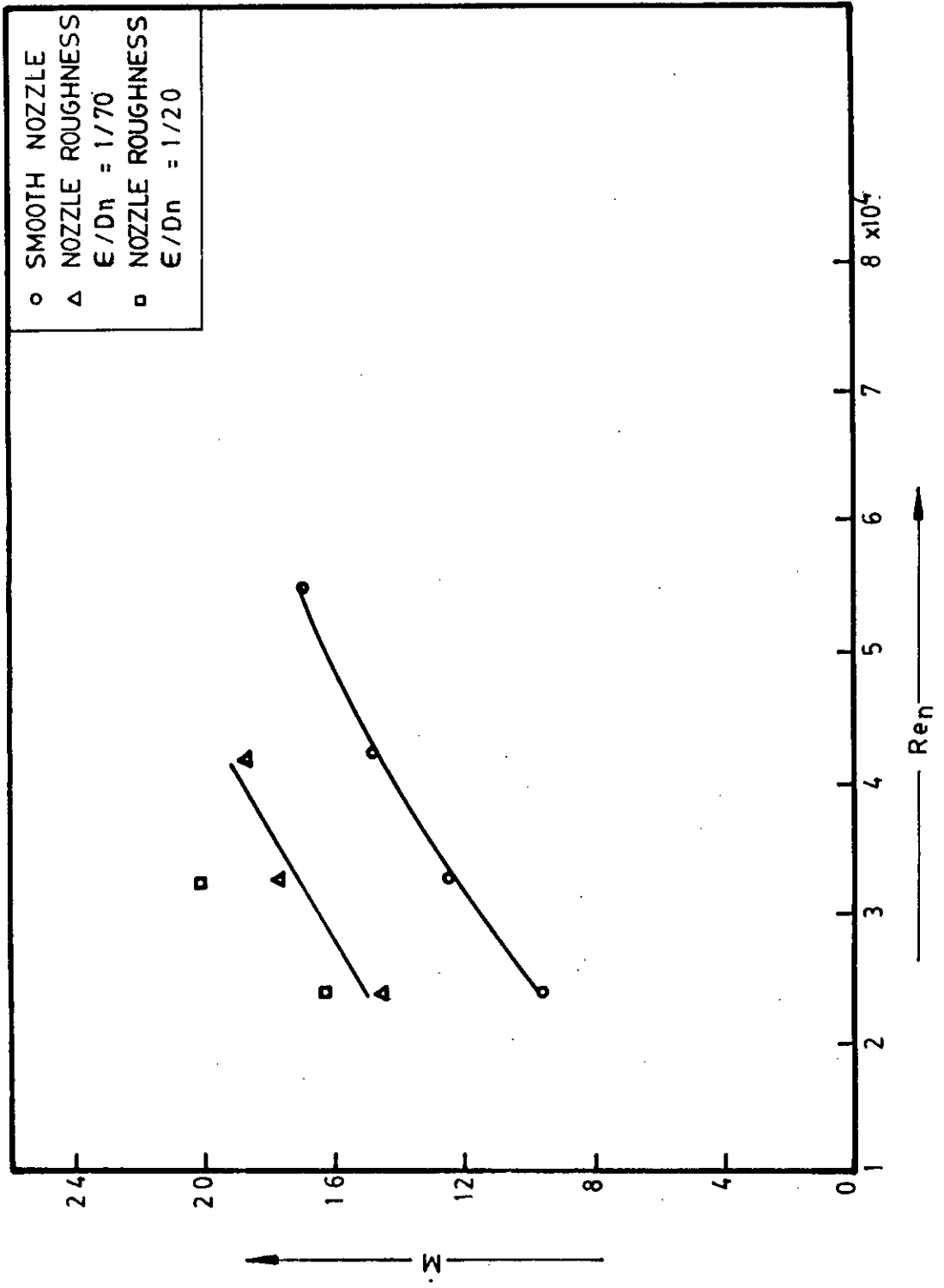


FIG. 5-14 RATE OF MASS ENTRAINMENT

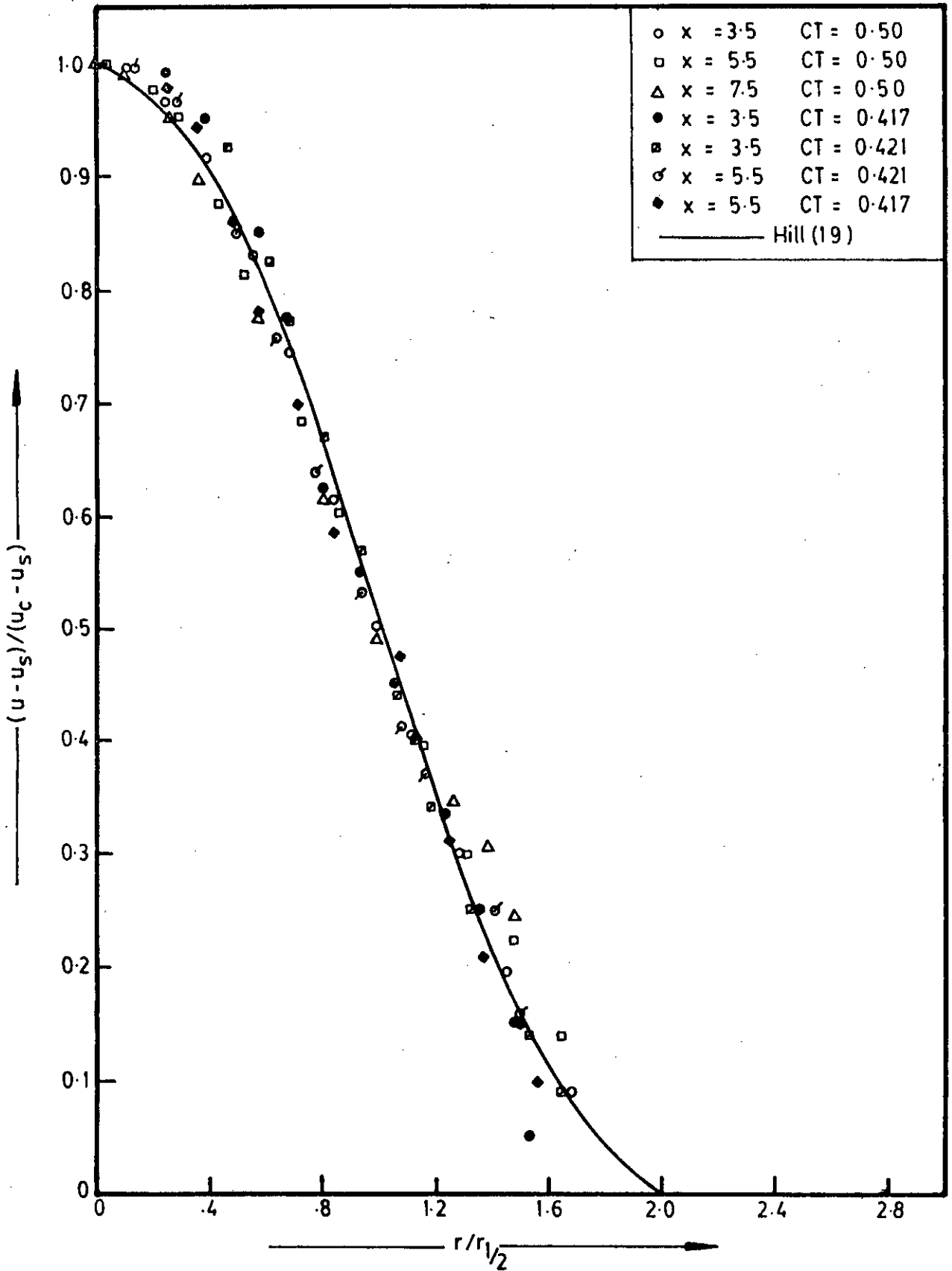


FIG. 5.15 EXCESS-VELOCITY PROFILE (SMOOTH NOZZLE)

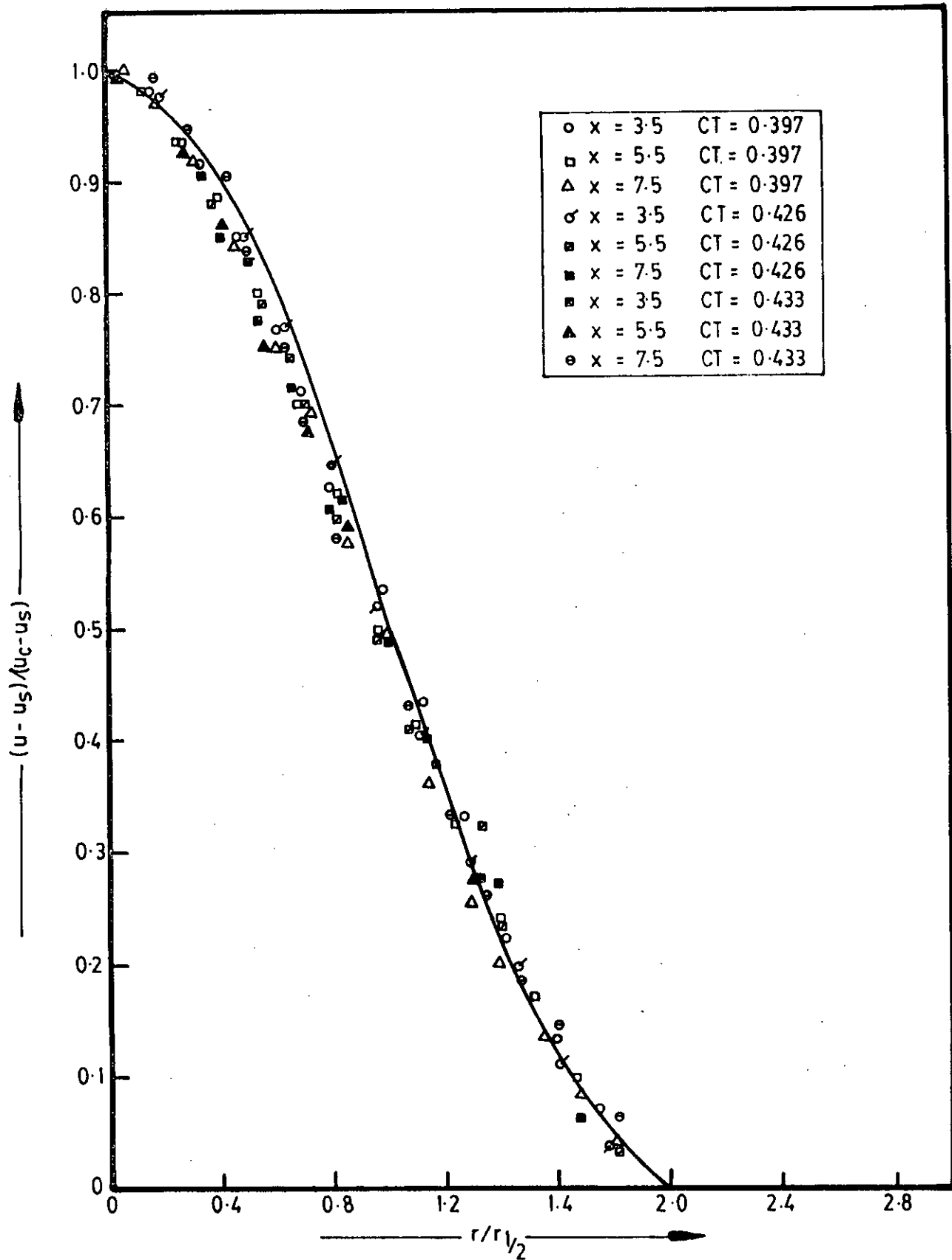


FIG-5.16 EXCESS-VELOCITY PROFILE (NOZZLE ROUGHNESS  $\epsilon/D_n=1/70$ )



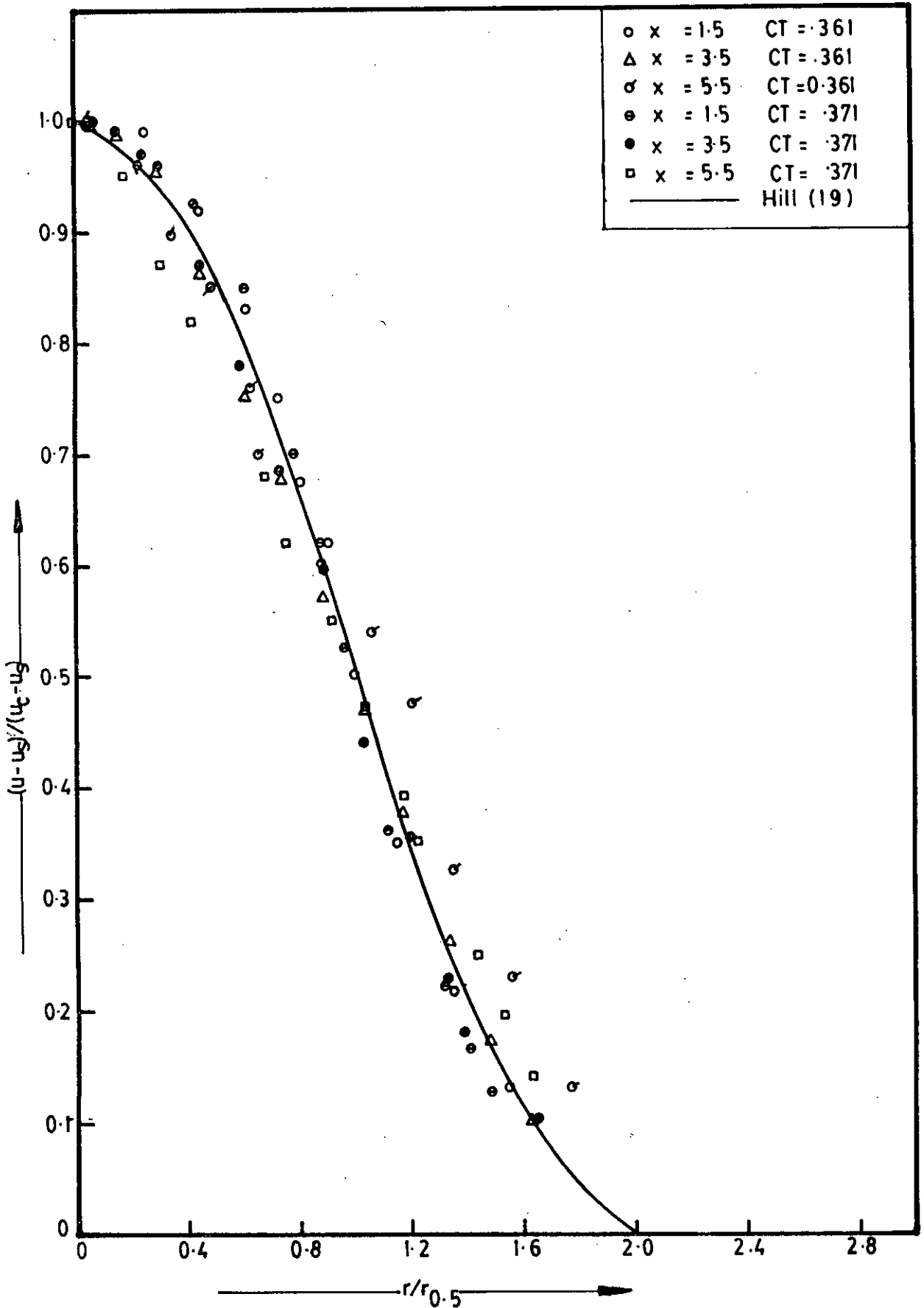


FIG. 5.17 EXCESS VELOCITY PROFILE (NOZZLE ROUGHNESS  $\epsilon/D_n = 1/20$ )

## LIST OF PLATES

<u>Plates</u>		<u>Page</u>
4.1	The Experimental Set Up	94
4.2	The Jet Producing Section	95
4.3	The Orifice Section	96
4.4	Packing Of Glass Tubes In The Settling Chamber	97
4.5	Close Up View Of Jet Nozzle	98
4.6	Instrumentation For Mean Quantity Measurements	99

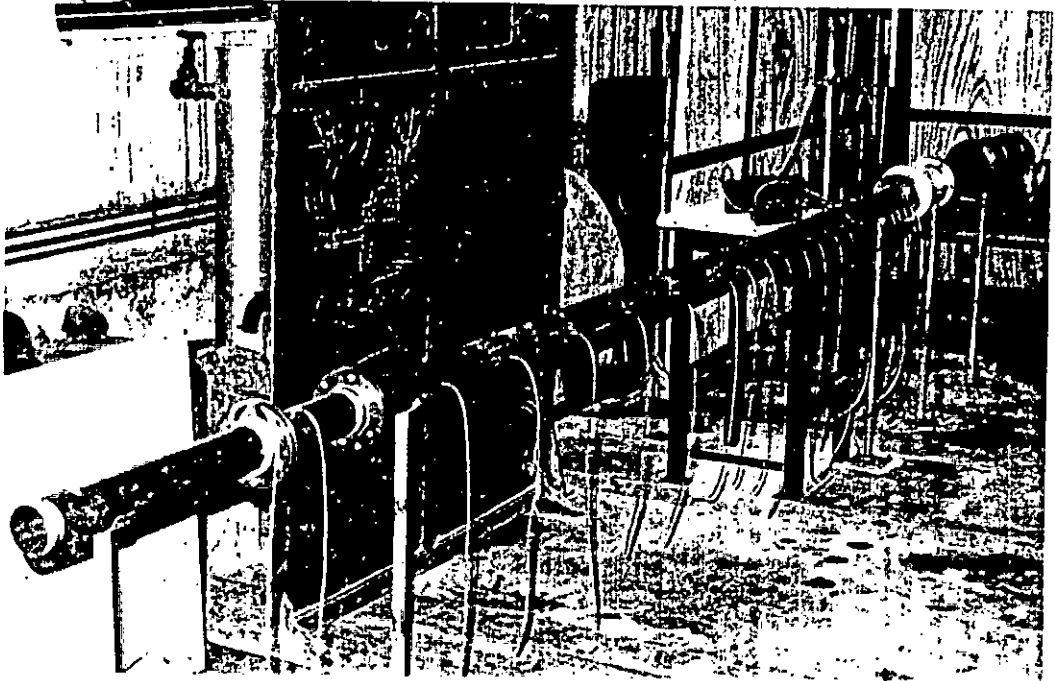


PLATE 4.1 , THE EXPERIMENTAL SET UP

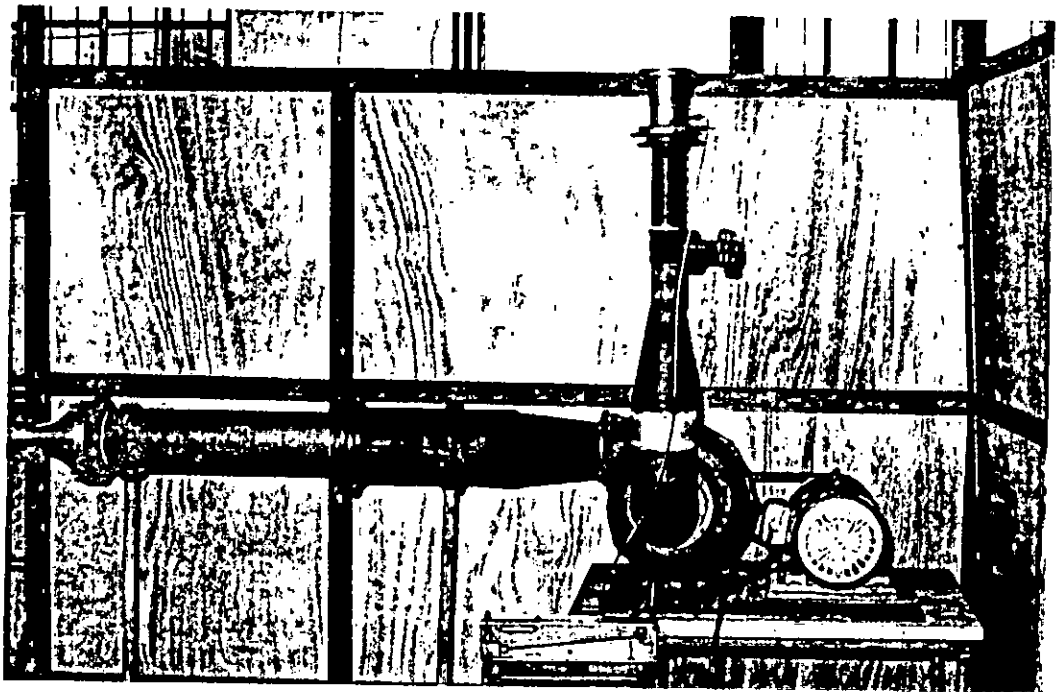


PLATE 4.2 THE JET PRODUCING SECTION

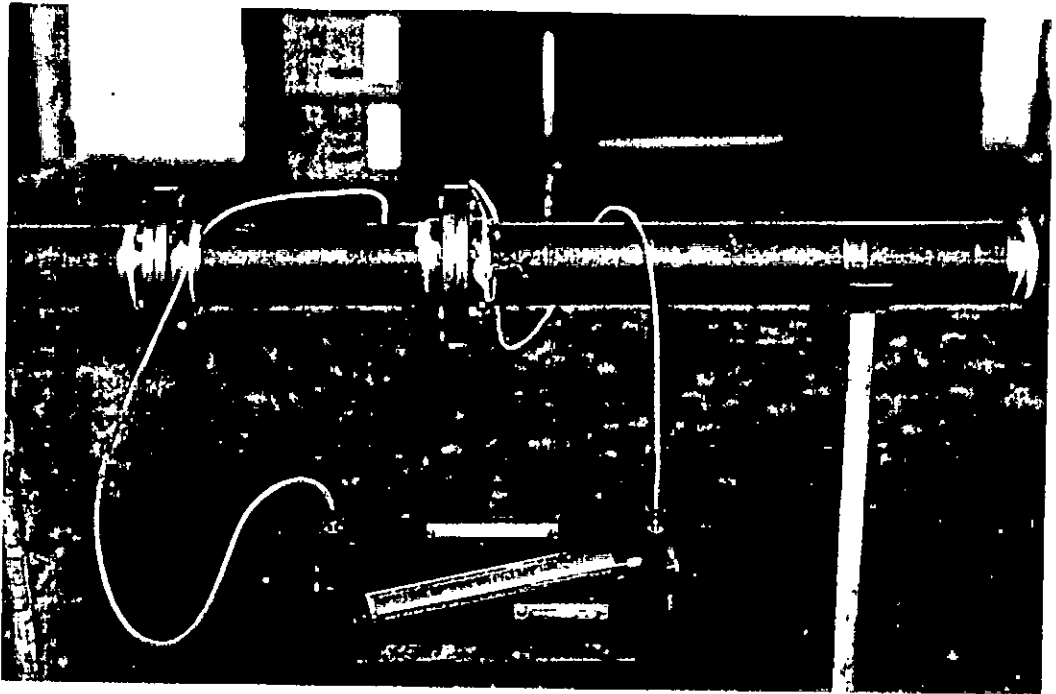


PLATE 4.3 THE ORIFICE SECTION

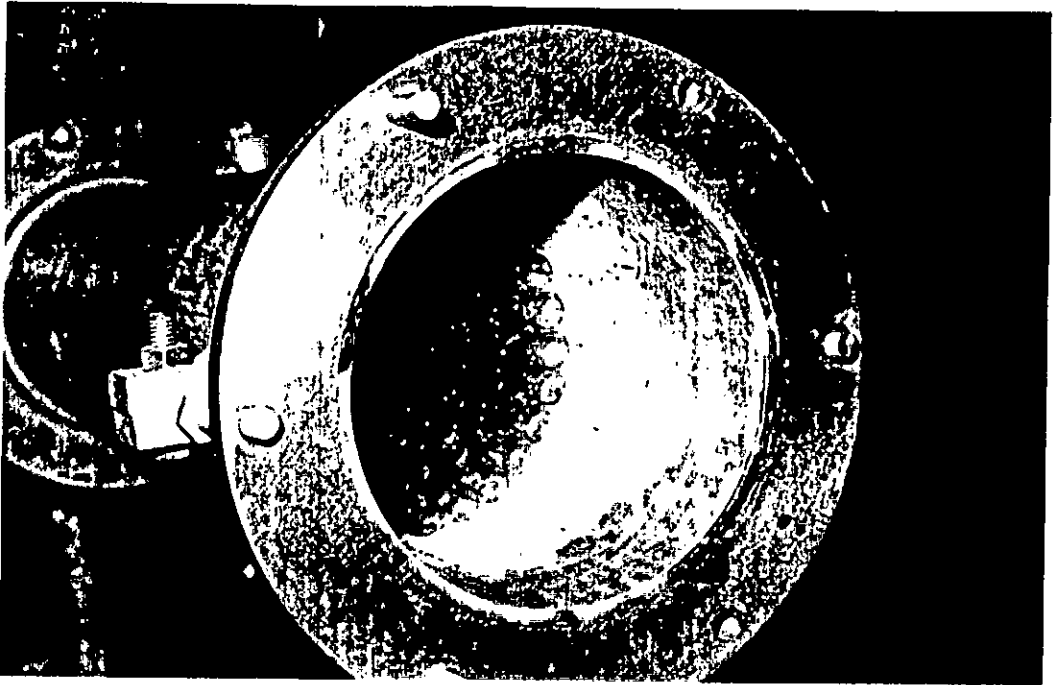


PLATE 4.4 PACKING OF GLASS TUBES IN THE SETTLING  
CHAMBER

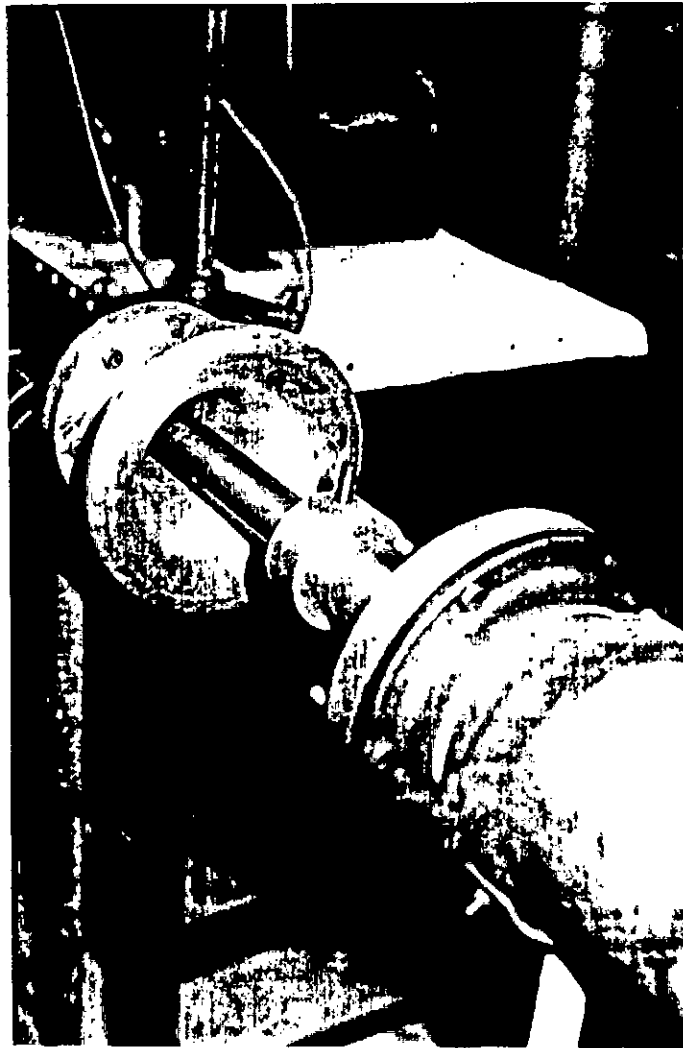


PLATE 4.5 CLOSE UP VIEW OF JET NOZZLE

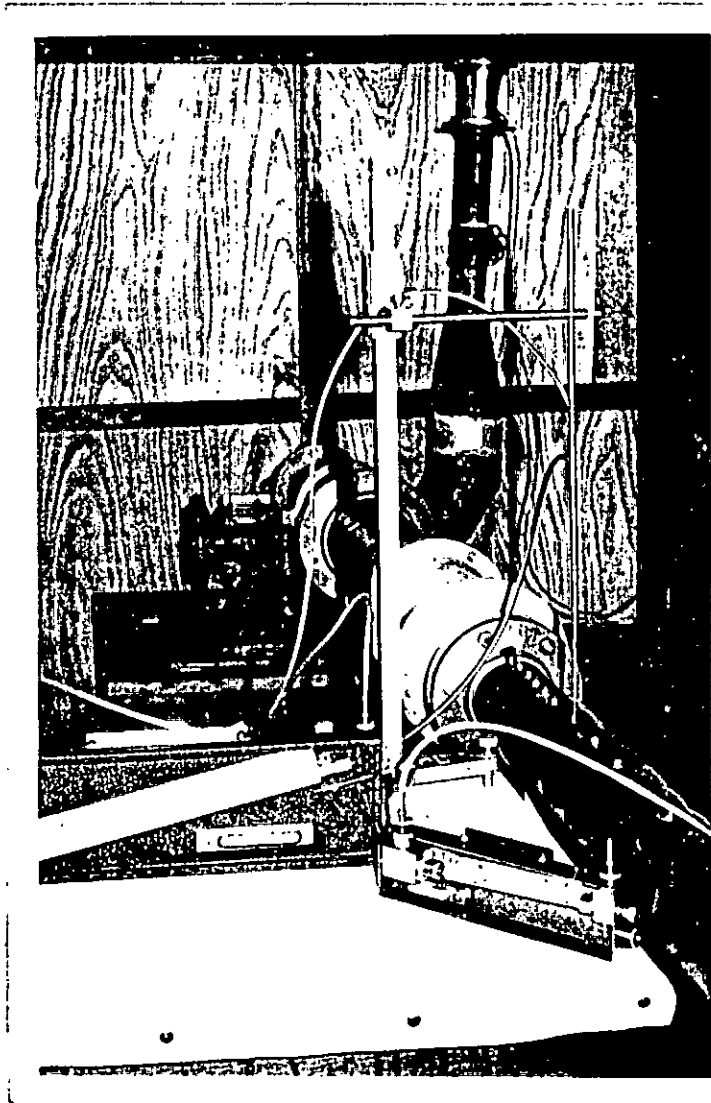


PLATE 4.6 INSTRUMENTATION FOR MEAN QUANTITY MEASUREMENTS

